CENTRAL RESEARCH LIBRARY

OAK RIDGE NATIONAL LABORATORY
OPERATED BY
UNION CARBIDE CORPORATION
NUCLEAR DIVISION

POST OFFICE BOX X
OAK RIDGE, TENNESSEE 37830

ORNL-MIT-206

DATE: December 17, 1974 COPY NO. 17

SUBJECT: Determination of ^{232}U Daughter Products Released from HTGR Fuel During Refabrication

AUTHOR: P.B. Jackson, H.H. Ficke, S.A. Reber, and C.I. Teich

Consultants: J.D. Jenkins, S.R. McNeany, J.E. Rushton, C. Hamby, Jr., R.L. Beatty, F.F. Dyer, and L.L. Fairchild

[redacted]

OAK RIDGE NATIONAL LABORATORY
CENTRAL RESEARCH LIBRARY
DOCUMENT COLLECTION
LIBRARY LOAN COPY
DO NOT TRANSFER TO ANOTHER PERSON
If you wish someone else to see this document, send in name with document and the library will arrange a loan.

ABSTRACT

During the refabrication of High Temperature Gas-Cooled Reactor (HTGR) fuel particles, uncoated resin beads loaded with ^{233}U are exposed to temperatures as high as 1700°C. Since ^{233}U fuels unavoidably contain trace quantities of ^{232}U, ^{232}U daughter products, such as ^{220}Rn and others, may evolve from the uncoated resin beads at high temperatures. Experiments with a ^{232}Th-loaded resin, rather than a ^{232}U-loaded resin, precluded shielding requirements because of the lower daughter product activity of ^{232}Th.

Below ^{228}Th the decay chains of ^{232}U and ^{232}Th are identical. The losses of decay chain species were investigated by monitoring the 583 and 2615 keV gamma emissions of ^{208}Tl. Computer-generated curves corresponding to various combinations of losses were compared to experimental data obtained at 400, 500, 600, 700, 800, 1000, and 1700°C. From 400-700°C the loss of ^{220}Rn was 100%, and losses of other species were not observed. At 800°C and above, the losses of ^{212}Pb and ^{212}Bi were significant. Loss of ^{212}Pb appears complete at 1000°C. A small percentage of ^{224}Ra was released at 1700°C, but no evidence of its release at lower temperatures was observed.

Oak Ridge Station
School of Chemical Engineering Practice
Massachusetts Institute of Technology

[redacted]

UCN-7802
(3 11-66)

Contents

Page

1. Summary 4
2. Introduction 5
   2.1 Background 5
   2.2 Objectives 8
   2.3 Method of Approach 8
   2.4 Theory 8
      2.4.1 Decay Theory 8
      2.4.2 Decay Equations for the ^{228}Th Decay Chain 10
      2.4.3 Bulk Properties of Nuclides 12
3. Apparatus and Procedure 13
   3.1 Thorium-Loaded Resin 13
   3.2 Carbonization and Conversion Furnace 14
   3.3 Gamma Detection Apparatus and Procedure 16
4. Results 18
   4.1 Theoretical Results 18
   4.2 Experimental Results 19
   4.3 Diffusion Modeling 29
5. Discussion 29
   5.1 Comparison of Thorium and Uranium Loaded Resins 29
   5.2 Comparison of Theoretical and Experimental Results 38
6. Conclusions 43
7. Recommendations 44
8. Acknowledgments 44
9. Appendix 45
   9.1 The Matrix Exponential Method for Solving Simultaneous Differential Equations 45
   9.2 Experimental Data 57
   9.3 Porosimetry Measurements 57
   9.4 Sample Calculations 57
   9.5 Location of Original Data 67
   9.6 Nomenclature 67
   9.7 Literature References 68

1. SUMMARY

Design of a fuel recycle and refabrication facility for the High Temperature Gas Cooled Reactor (HTGR) requires attention to the possibility of radioactive off-gas discharge. Such losses might occur when resin beads loaded with recycled ^{233}U and trace ^{232}U contaminant are carbonized and converted at high temperatures to a uranium oxide and uranium carbide mixture. These processes may cause release of daughter products in the ^{232}U decay chain into process gas streams.

The uranium fuel was simulated using resin loaded with ^{232}Th thereby eliminating the need for extensive shielding during experimentation. This substitution was possible because the decay chains of ^{232}U and ^{232}Th are identical after ^{228}Th. Resin beads were heated to various temperatures in a fluidized conversion furnace at 10°C/min and held at the final temperature for four hours. Each run was assumed to have been conducted at a constant temperature. Losses were measured by monitoring the 583 and 2615 keV gamma activity of the daughter ^{208}Tl as it decays to ^{208}Pb with a Ge-Li detector. Plots of theoretical ^{208}Tl activity were generated using the MATEXP computer program for various losses of the decay species by employing a forcing function corresponding to species removal. A typical plot showed the ^{208}Tl activity decreasing with time, reaching a minimum, and then gradually returning to secular equilibrium. It was found that the depth of the generated well was a function of the quantity of species lost, while the shape of the response curve was determined by the identity of the species lost. The experimental curves and the computer simulations were compared to determine the extent and composition of the off-gas losses.

Approximately 100% loss of ^{220}Rn was observed at temperatures of 400-700°C. However, losses in this range varied inversely with temperature with a maximum 8% deviation between observed and predicted values. This deviation cannot be explained by experimental error. The experimental observations may be due to changes in resin structure with temperature. Nitrogen adsorption measurements are recommended to characterize the resin structure. The discrepancy in the 400-700°C experiments can be overcome by rerunning the experiments with precarbonized resin. At 800°C the experimental curve was fitted to a model based on 100% loss of ^{220}Rn, and some loss of ^{212}Pb and ^{212}Bi. At 1000°C the experimental data could not be fitted to the simple computer model. Significantly higher losses of ^{212}Pb and ^{212}Bi indicate a mechanism more complex than the immediate removal of a single species.

Two runs were conducted under the conditions used in the actual refabrication process. It was found in the simulation of the carbonization step run at 2°C/min to 600°C that approximately 100% of the ^{220}Rn was lost, accompanied by some ^{212}Bi. When the beads were heated at 90°C/min to 1700°C, simulating the conversion step, some ^{224}Ra was lost with ^{212}Pb, ^{212}Bi, and ^{220}Rn. No other evidence of ^{224}Ra losses was observed in this investigation.

2. INTRODUCTION

2.1 Background

ORNL is presently designing a High Temperature Gas Cooled Reactor (HTGR) fuel recycle and refabrication pilot plant. A commercial facility would serve a group of 20,000 MW HTGRs and process 40 kg of ^{233}U (or 400 kg of heavy metal) per day (4). To determine the procedures and equipment necessary to establish a commercial HTGR fuel refabrication plant, a pilot facility is currently being designed. The pilot facility will be capable of handling 25 kg of heavy metal per day, corresponding to 2.5 kg of ^{233}U (4).

Spent HTGR fuel elements will be chemically reprocessed to remove accumulated fission products which act as neutron poisons. The remaining uranium will be refabricated into new fuel elements and recycled back into an HTGR. Figure 1 shows how ^{232}U is formed in a reactor and also the natural decay chains of ^{232}U and ^{232}Th.

Figure 2 is a schematic of the proposed refabrication pilot plant. The daughter products are separated in System 1 by ion exchange and solvent extraction, and a fresh feed solution of uranyl nitrate $[UO_2(NO_3)_2 \cdot 6H_2O]$ is prepared. The uranium is loaded onto weak acid resin beads in System 2 by contacting the resin and uranyl nitrate solution. The loaded resin is then dried and passed to an argon fluidized furnace (System 3) where it is heated at 2°C/min to 600°C to decompose the constituent hydrocarbons and drive off volatile matter. In System 4 another furnace heats the material at 87.5°C/min (3) to 1700°C to partially convert the UO_2 to UC_2. The furnace temperature is then lowered to 1200°C, and protective coatings of carbon and silicon-carbide are applied. These coatings are impervious to gases and thus prevent subsequent escape of radioactive gases.

In System 5 the coated beads are blended with thorium oxide coated particles and injected with heated pitch and graphite to form fuel "green rods." The rods are loaded into graphite fuel blocks which are subsequently carbonized and cleaned in System 6. Product quality control is maintained in Systems 7 and 8. Systems 9 and 10 are waste and material handling, respectively.

Concern exists that during the carbonization and conversion steps, Systems 3 and 4, two of the ^{232}U daughter products, ^{220}Rn and ^{224}Ra, may leave fuel kernels in the argon off-gas stream, thereby creating the need for an off-gas ventilation system to handle the radioactive ^{224}Ra and ^{220}Rn gases. The rates of release during the carbonization and conversion steps must be investigated for design of such an off-gas system.

All reactor fuel rods which contain ^{233}U invariably contain some ^{232}U at estimated concentrations between 100 and 1500 ppm (4). In Figure 1 ^{232}U is shown to decay to ^{228}Th with a half-life of 72 yr. However, ^{228}Th also appears in the decay chain of ^{232}Th with ^{228}Ra and ^{228}Ac as intermediates. The long half-life of ^{232}Th, 1.39×10^{10} yr, when compared to

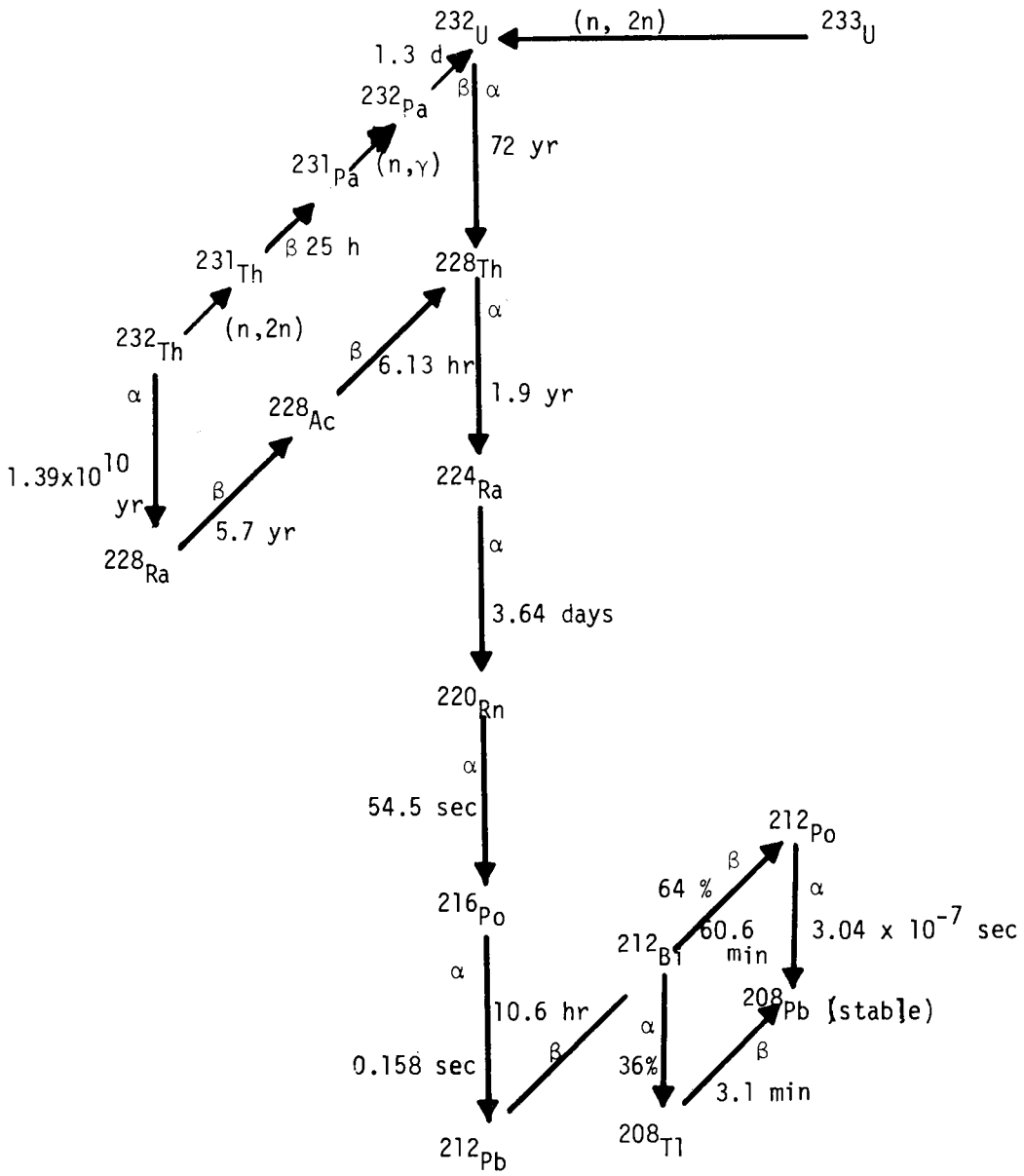

MASSACHUSETTS INSTITUTE OF TECHNOLOGY
SCHOOL OF CHEMICAL ENGINEERING PRACTICE
AT
OAK RIDGE NATIONAL LABORATORY

^{232}U AND ^{232}Th DECAY CHAIN (4)

DATE	DRAWN BY	FILE NO.	FIG.
12-16-74	PBJ	CEPS-X-206	1

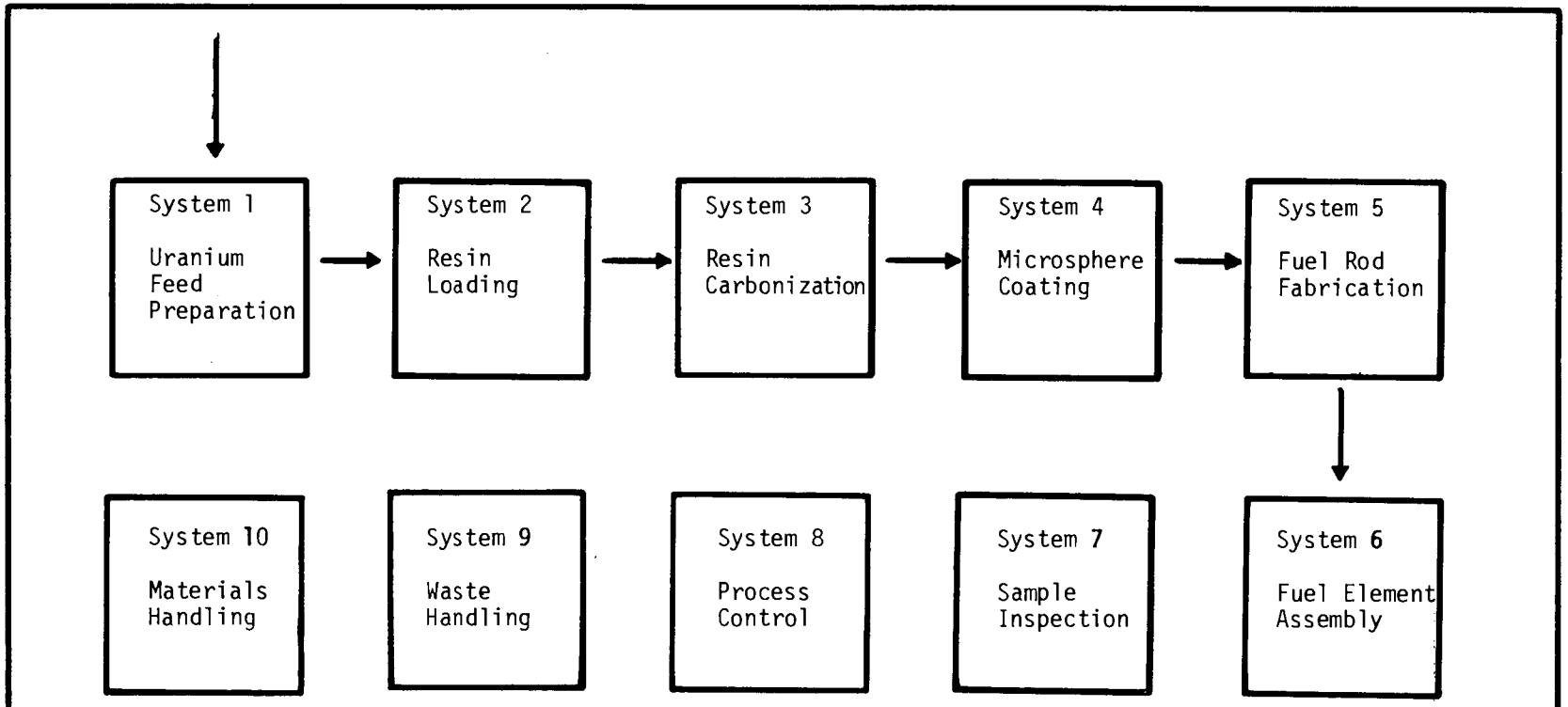

MASSACHUSETTS INSTITUTE OF TECHNOLOGY
SCHOOL OF CHEMICAL ENGINEERING PRACTICE
AT
OAK RIDGE NATIONAL LABORATORY

PROPOSED HTGR FUEL REFABRICATION
PILOT PLANT SYSTEMS

DATE	DRAWN BY	FILE NO.	FIG.
12-16-74	PBJ	CEPS-X-206	2

that of ^{232}U, 72 yr, indicates that higher concentrations of ^{228}Th are expected from ^{232}U decay than from ^{232}Th decay, and therefore necessitates gamma radiation shielding. ^{228}Th decays to ^{224}Ra with a half-life of 1.9 yr and proceeds through several other radioactive intermediates to a stable ^{208}Pb isotope. All of the species after ^{228}Th have shorter half-lives than ^{228}Th; so, a secular equilibrium is created between ^{228}Th and ^{208}Tl after approximately 30 days. A change in the rate of decay of any species in the chain can be detected by observing the high-energy ^{208}Tl gamma emission at 2.61 Mev. Hence, loss of any species in the decay chain can also be determined from the ^{208}Tl gamma emission.

2.2 Objectives

The objectives were to determine the effects of furnace temperature on quantities of ^{224}Ra and ^{220}Rn released, to investigate the release of other radioactive species, and to develop mathematical models to predict the off-gas generation rates at various temperatures.

2.3 Method of Approach

To meet the objectives the following plan of attack was proposed:

1. Determine whether beads agglomerate at high rates of heating (10-40°C/min) during carbonization. High heating rates would allow rapid attainment of the desired temperature, thus allowing a steady state investigation of diffusion limitations.

2. Modify the MATEXP (1) program for solving ordinary differential equations to calculate ^{220}Rn, ^{224}Ra, and other species' concentrations for various given off-gas release rates. The ordinary differential equations for decay of each species in the decay chain must be set up and initial conditions obtained by assuming secular equilibrium before heating.

3. Determine a set of temperatures from the carbonization temperature range of 600-1700°C at which to conduct experiments.

4. Obtain experimental data for ^{220}Rn and ^{224}Ra losses at various temperatures.

2.4 Theory

2.4.1 Decay Theory

Nuclides usually decay in three ways:

1. Alpha decay, with the emission of an alpha particle, a doubly charged He nucleus:

$$\text{e.g.,}\ {}^{239}Pu_{94} \longrightarrow {}^{235}U_{92} + {}^{4}He_{2}$$

2. Beta decay, causing the emission of an electron:

$$\text{e.g.,}\ {}^{89}Sr_{38} \longrightarrow {}^{89}Y_{39} + {}^{0}\beta_{-1}$$

3. Gamma emission, i.e., electromagnetic radiation emitted at a characteristic frequency when a nucleus undergoes the transition from a state of higher energy to one of lower energy.

The rate of radioactive decay is determined by the decay constant, λ, which is independent of temperature, pressure, and the decay of neighboring nuclei. Radioactive decay is analogous to a first-order chemical reaction since the decay rate is proportional to the number density (concentration), N; hence,

$$\frac{dN}{dt} = -\lambda N$$

In integrated form,

$$N = N_o\, e^{-\lambda t}$$

The half life of a nuclide, $t_{\frac{1}{2}}$, is defined as the length of time needed for half the original nuclide to decay. Therefore,

$$\frac{N_o}{2} = N_o\, e^{-\lambda t_{\frac{1}{2}}}$$

and

$$t_{\frac{1}{2}} = \frac{\ell n 2}{\lambda}$$

For the decay chain P $\rightarrow$ D $\rightarrow$ other products, the following is true:

$$\frac{d[D]}{dt} = \lambda_P[P] - \lambda_D[D]$$

that is, the rate of change of concentration of D equals the generation of D minus the decay of D. If the half-life of a parent nuclide is long compared with those of its daughters, then a secular equilibrium or steady state is attainable. At secular equilibrium the change in concentration with respect to time is zero for all species in the decay chain. Thus, the ratios of their concentrations can be calculated from their half-lives.

2.4.2 Decay Equations for the ^{228}Th Decay Chain

The decay chain of the ^{232}U impurity, which is contained in the ^{233}U HTGR fuel, is shown in Fig. 1 to be identical to the decay chain of ^{232}Th after the common daughter product, ^{228}Th. To facilitate the study of radioactive gas release from the fuel particles during reprocessing, a mathematical simulation of the decay scheme has been developed. The simulation includes the ^{232}Th daughter products from ^{228}Th through ^{208}Tl. The half-lives of ^{228}Th and ^{224}Ra are 1.9 yr and 3.64 days, respectively. Therefore, small changes in the ^{228}Th concentration due to decay during the time period of experimentation, approximately one week, have little effect and may be neglected. A condition of secular equilibrium exists in the decay chain resulting in essentially constant concentrations of all species from ^{228}Th through ^{208}Tl. Differential mass balances may be written for each species to describe the overall decay scheme. Constant forcing functions are included to allow perturbation of the set of equations to simulate the loss of various percentages of the species during carbonization. During this analysis, ^{216}Po has been neglected as a member of the decay family because of its half-life, 0.158 sec. The decay chain may be approximated by ^{220}Rn decaying instantaneously to ^{212}Pb; thus, calculational difficulties caused by the short half-life of ^{216}Po are avoided (see Appendix 9.1 for additional discussion).

Therefore, the decay may be described by the following set of equations:

$$\frac{d[^{228}Th]}{dt} \cong 0.0 \tag{1}$$

$$\frac{d[^{224}Ra]}{dt} = \lambda_{Th}[^{228}Th] - \lambda_{Ra}[^{224}Ra] + Z(A) \tag{2}$$

$$\frac{d[^{220}Rn]}{dt} = \lambda_{Ra}[^{224}Ra] - \lambda_{Rn}[^{220}Rn] + Z(2) \tag{3}$$

$$\frac{d[^{212}Pb]}{dt} = \lambda_{Rn}[^{220}Rn] - \lambda_{Pb}[^{212}Pb] + Z(3) \tag{4}$$

$$\frac{d[^{212}Bi]}{dt} = \lambda_{Pb}[^{212}Pb] - \lambda_{Bi}[^{212}Bi] + Z(4) \tag{5}$$

$$\frac{d[^{208}Tl]}{dt} = (0.36)\lambda_{Bi}[^{212}Bi] - \lambda_{Tl}[^{208}Tl] + Z(5) \qquad (6)$$

Z(A) and Z(2) through Z(5) are forcing functions which correspond to net removal of the species by mass transfer out of the fuel bead. As a consequence of Eq. (1), the ^{228}Th term in Eq. (2) may be expressed as a constant value.

$$Z(B) = \lambda_{Th}[^{228}Th]$$

Therefore, an overall Z can be defined in Eq. (2):

$$Z(1) = Z(B) + Z(A)$$

Equation (2) then reduces to

$$\frac{d[^{224}Ra]}{dt} = -\lambda_{Ra}[^{224}Ra] + Z(1) \qquad (7)$$

At secular equilibrium, the differential terms and forcing functions in Eqs. (2) through (6) become zero, and the following conditions exist:

$$\lambda_{Th}[^{228}Th] = \lambda_{Ra}[^{224}Ra] = \lambda_{Rn}[^{220}Rn] = \lambda_{Pb}[^{212}Pb]$$

$$= \lambda_{Bi}[^{212}Bi] = 2.78\ \lambda_{Tl}[^{208}Tl] \qquad (8)$$

Thus, from the known values of the decay constants, initial conditions corresponding to the secular equilibrium values may be calculated relative to a fixed ^{208}Tl concentration. A step-function decrease to a fixed species concentration is arbitrarily chosen as a forcing function. By means of this forcing function, the species concentration is decreased from its initial secular equilibrium value to a fixed percentage of the value and is maintained at this fixed value for some length of time. This concentration profile imposed numerically for any chosen species by decreasing instantaneously the initial value of the species concentration to the fixed value and by adding at the same time a constant valued forcing function, Z, to make the right hand side of the species mass balance become zero. Thus, "A 25% loss of ^{220}Rn" in the analytical model means that ^{220}Rn concentration was decreased from its secular equilibrium value to 75% of that value and maintained at that level for some length of time. Once values for the forcing functions are supplied, the five-equation matrix can be solved to determine the concentration profile as a function of time for each decay chain species. A detailed description of the solution technique is in Appendix 9.1.

The shape of the ^{208}Tl concentration profile will vary depending on which species above ^{208}Tl in the decay chain is being removed. The different half-lives of the decay chain elements cause variations in the effects the individual constant forcing functions have on the ^{208}Tl profile. For instance, the simulated removal of ^{220}Rn by the forcing function Z(2) produces a slow decrease in ^{208}Tl concentration because ^{212}Pb, with a relatively long half-life, moderates the forcing function's effect. If, however, ^{212}Bi were removed, a relatively instantaneous effect on the ^{208}Tl concentration will occur. Therefore, ^{208}Tl profiles can be generated for various combinations of forcing functions imposed for periods corresponding to the experimental heating period. These profiles can then be compared to the experimentally determined ^{208}Tl profiles to obtain an estimation of the types and quantities of species lost.

2.4.3 Bulk Properties of Nuclides

An order of magnitude calculation, shown in Appendix 9.4, was performed to determine the equilibrium concentrations of ^{208}Pb and ^{218}Bi in the ^{232}Th loaded resin beads. The concentrations were found to be 2.04×10^{-20} and 1.94×10^{-21}, moles/bead, respectively. At such low concentrations, bulk physical properties such as melting point, boiling point, and vapor pressure have little meaning. It was hoped that investigation into the chemical reactivity of the nuclides involved in the decay chain would provide some insight as to why a particular species might perferentially leave the resin. A literature survey indicates that BiO_2 has been prepared commercially by passing oxygen streams over the molten metal at elevated temperatures (7). PbO forms in the presence of moist air. Since argon is used in the fluidized carbonization furnace, oxygen can be evolved only from $ThO_2(NO_3)_2$ and the resin, $C_6H_6O_2$. Standen (7) cites no Tl-C, Bi-C, Pb-C, Ra-C, or Rn-C compounds; however, Th-C_2 is formed by reacting ThO_2 with carbon at approximately 1400°C. Therefore, it is unlikely that the radioactive decay species indicated in Fig. 1 will form stable carbon compounds. Since Pb, Bi, Po, and Tl show similar melting points as in Table 1, one might suspect that evolution of these species may occur at similar temperature.

Table 1. Melting and Boiling Point Data (9)

Species	Melting Point (°C)	Boiling Point (°C)
Th	1700	4000
Ra	700	1140
Rn	-71	-62
Po	254	962
Pb	328	1744
Bi	271	1560
Tl	304	1457

3. APPARATUS AND PROCEDURE

3.1 Thorium Loaded Resin

Weak cation exchange resin beads (Rohm & Haas, IRC-72, $C_6H_6O_2$) were loaded with ^{232}Th along with some ^{228}Th impurity from a solution of thorium nitrate approximately one month before this study was conducted. At that time, the ^{232}Th was more than ten years old, and an equilibrium had been established between ^{228}Th and all daughter products. After loading the thorium onto the beads, the equilibrium between ^{228}Th and its daughter products was probably destroyed, but the $^{232}Th/^{228}Th$ ratio remained the same due to the equivalent chemical nature of thorium isotopes. Within ten half lives, 36.5 days, radium concentration returns to an equilibrium value; and, since all of its daughter products have half lives shorter than 3.65 days, they also can be assumed to be in equilibrium after 36.5 days. A mass balance on ^{224}Ra yields

$$\frac{d[^{224}Ra]}{dt} = \lambda_{Th}[^{228}Th] - \lambda_{Ra}[^{224}Ra] \tag{9}$$

According to Eq. (1),

$$\frac{d[^{228}Th]}{dt} = 0$$

Therefore,

$$\frac{d[^{224}Ra]}{dt} + \lambda_{Ra}[^{224}Ra] = K$$

where:

$$K = \lambda_{Th}[^{228}Th]$$

Equation (9) is a first order linear differential equation which can be solved with the use of an integrating factor, $\exp[\lambda_{Ra}\ t]$. Multiplying Eq. (9) by the integrating factor and integrating yields:

$$[^{224}Ra]\ \exp(\lambda_{Ra}\ t) = \int[e^{\lambda_{Ra}t}Kdt] + C \tag{10}$$

Hence the concentration of radium at any time, t, is governed by the exponential term which includes only the ^{224}Ra decay constant and not the ^{228}Th decay constant. We can therefore assume the amount of ^{228}Th on the beads at 36.5 days to be in equilibrium with the ^{224}Ra and the other members of the decay chain.

3.2 Carbonization and Conversion Furnace

A diagram of the furnace is found in Fig. 3. The furnace which operates as a fluidized bed is encased in an outer, water-cooled, aluminum shell. A graphite tube within this shell serves as a heating and fluidization chamber. When a voltage is applied across the tube, electrical power dissipation heats the tube and its contents. The rate of heating is controlled by a temperature relay and is programmed prior to an experiment. Temperature is monitored with a chromel-alumel thermocouple. The bed is fluidized by a flow of argon gas through the tube. Bed fluidization is maintained by adjusting the gas volumetric flow rate. Exit gases from the furnace flow through an activated carbon bed, a series of gauze filters, and the building scrubber system. At the end of the heating period, the electric power is turned off, and the sample is cooled by the continuing flow of argon through the tube. The gas flow is then shut off, and the sample dropped through a conical adapter to an attached sample container. The magnesium sample container is removed from the apparatus, capped under argon, and transported to the detection system facility.

The amount of resin used in each batch was 18 g, the amount required to completely fill any magnesium sample container. The resin was shape separated prior to any experimental runs. The programmed temperature rate used to heat the particles was as high as the particles could tolerate without evidence of significant damage; this was found to be 10°C/min. Estimates of particle damage were made using an optical microscope with a magnification of 6X.

The following steps were performed for each experiment. Eighteen grams of resin were weighed out to ± 0.01 g. The electric power and argon were turned on, and the sample poured into the graphite tube. The sample remained in the furnace for the warmup time (the time until the furnace could be heated at 12°/min) plus the time needed to reach the desired temperature, plus the length of time the sample was to be kept at that temperature. As the temperature of the furnace changed, the volumetric flow rate of the argon was modified to maintain a constant mass flow rate of gas through the furnace. When the run was over, the electric power was turned off, and the sample gas-cooled for 20-30 min. After cooling, the sample and container were weighed, placed in a plastic bag, inspected and tagged by a Health Physics Officer, and taken to the Ge-Li detector system for monitoring.

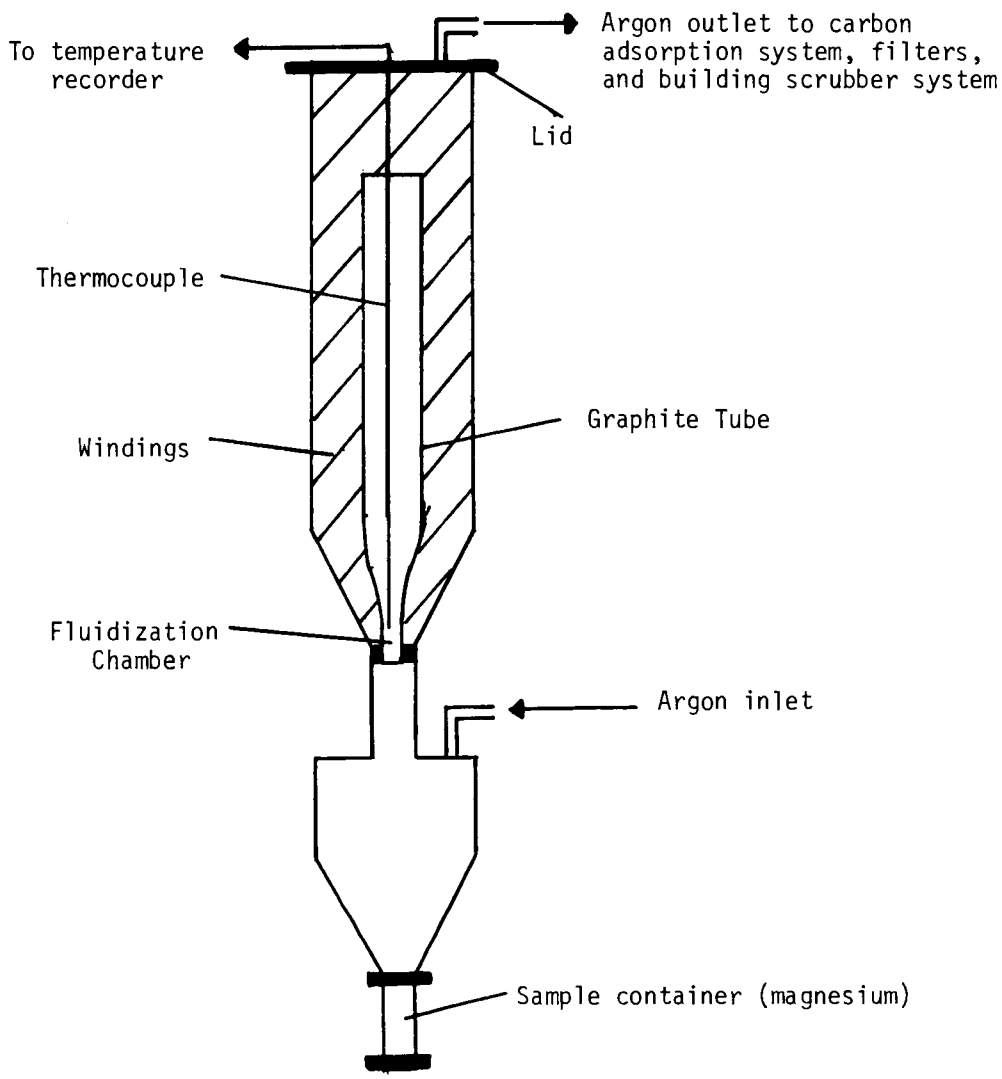

MASSACHUSETTS INSTITUTE OF TECHNOLOGY
SCHOOL OF CHEMICAL ENGINEERING PRACTICE
AT
OAK RIDGE NATIONAL LABORATORY

EXPERIMENTAL APPARATUS - GRAPHITE RESISTANCE FURNACE

DATE	DRAWN BY	FILE NO.	FIG.
12-16-74	SAR	CEPS-X-206	3

3.3 Gamma Detection Apparatus and Procedure

A schematic of the gamma detection system is presented in Fig. 4. The Ge-Li detector is housed in a lead brick enclosure and is shielded from alpha and beta radiation by a beryllium plate. Whenever a gamma ray strikes the detector, a pulse of energy proportional to the incident gamma energy is produced. The pulse is amplified, then converted to a digital signal in a combination-multichannel analyzer-analog-digital converter (ADC-ADD1 unit). The ADC-ADD1 unit measures the energy of the pulse and converts it to a digital signal which causes the number of counts in the proper energy channel to be augmented by one. In this manner a gamma ray histogram, or spectrum, is produced.

The detection system is interfaced with a PDP-11 computer programmed to analyze the spectrum. The counts between peak boundaries are summed and a linear baseline formed. The net number of counts due to the gamma-emitting sample is determined as:

$$\text{counts/second (cps)} = \text{net counts/counting time}$$

This value must be corrected for geometric reasons and for the detector efficiency:

$$\text{gamma activity} = \text{cps(geometric factor/detector efficiency)}$$

The geometric factor is a function of the distance between the Ge-Li detector and the sample. Since gamma rays travel in straight lines, only a fraction of the total gamma rays emitted, proportional to $1/(\text{distance})^2$, strike the detector. Thus, the geometric factor corrects for the solid angle through which gamma photons are emitted without encountering the detector.

The detection efficiency is a function of both gamma ray energy and distance between sample and detector. It is usually determined by recording the cps for a standard radioactive sample at all desired wavelengths and at the distance which is to be used. Wavelength affects the efficiency because the amount of gamma ray absorption by the sample itself varies with the gamma ray energy; gamma photons of higher energy more easily penetrate the sample.

The computer is also programmed to calculate an estimate of the statistical error in determining the number of counts per second. The error was in the range of 2-5% with 99.73% confidence or three standard deviations for all samples observed.

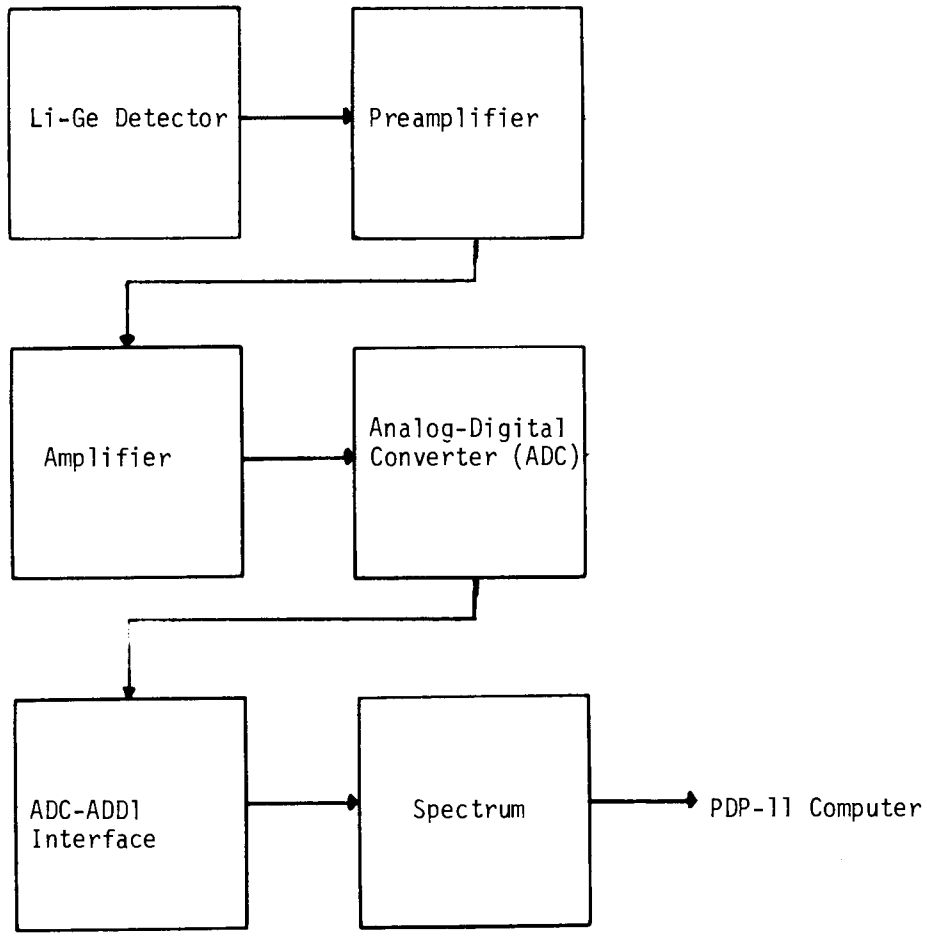

MASSACHUSETTS INSTITUTE OF TECHNOLOGY
SCHOOL OF CHEMICAL ENGINEERING PRACTICE
AT
OAK RIDGE NATIONAL LABORATORY

SCHEMATIC OF DETECTION SYSTEM

DATE	DRAWN BY	FILE NO.	FIG.
12-17-74	PBJ	CEPS-X-206	4

The counting procedure used two gamma energies, 583 and 2615 keV, corresponding to ^{208}Tl activity, and included a background count taken on an empty 4.5 cc magnesium sample container. After heating a batch of thorium-loaded resin in the furnace, the beads were cooled, transferred to the container as quickly as possible, and transported to the detection system. A minimum of one-half hour elapsed between the time when the furnace was turned off and the first count was recorded. The activity was monitored continuously throughout the night following the experimental run. The detection system was capable of counting for any desired time interval, then immediately beginning the next count after printing out the previous one. Twelve minutes was chosen as the counting interval since the error per count at 99% confidence was more than 10% at shorter times. Counting at 12-min intervals throughout the night yielded approximately eighty data points per experimental run.

Since the relative ^{208}Tl activity, a percentage of its secular equilibrium value, was desired, the sample was allowed to return to equilibrium while sample activity was monitored until it did not change significantly over a two-day period. If the return to equilibrium was controlled by ^{208}Pb, with a half-life of 10.6 hr, seven half-lives, or 74 hr, was required to attain steady state. The activity of an unheated sample at secular equilibrium cannot be used as a reference because its density, and hence its self-shielding ability, is much less than that for a carbonized sample. Carbonized sample density was approximately 2 g/cm^3 as compared with 1 g/cm^3 for the unheated beads.

Since relative ^{208}Tl activity only was required in this study, absolute gamma emission data were not taken. All observed values of activity were divided by the same arbitrary detector efficiency, so no error was induced when comparing relative thallium activities. To back-calculate absolute concentrations of species in the decay chain using thallium activity alone is impossible because of the arbitrary efficiency.

4. RESULTS

4.1 Theoretical Results

Computer simulations have been carried out to determine the response of the ^{228}Th decay chain to the removal of various chain species. In each computer simulation a single species has been depleted to 50% of its value at time zero and held constant for four hours by the application of the appropriate forcing function as explained in Sect. 2.4.1. After the 4-hr period which corresponds to the bead heating period, the forcing function was set to zero and the decay chain allowed to approach secular equilibrium.

Computer-generated curves which indicate ^{208}Tl activity for losses of ^{224}Ra, ^{220}Rn, ^{212}Pb, and ^{212}Bi, respectively, are illustrated in Figs. 5, 6, 7, and 8. It is shown in Fig. 5 that if ^{224}Ra is removed, the return to equilibrium would occur after several days due to the relatively long ^{224}Ra half-life. In fact, after one week secular equilibrium would not have been established, and the relative ^{208}Tl concentration would not have returned to 100%.

In Fig. 6 the effect of a 50% ^{220}Rn release on the species below it in the chain is seen to be identical with that of ^{224}Ra release during the 4-hr depletion period. The short half-life of ^{220}Rn, however, allows rapid return to secular equilibrium, determined by the undisturbed ^{224}Ra concentration, when the forcing function is removed. The species below ^{220}Rn in the decay chain then return to secular equilibrium after a time lag which is proportional to the intervening species' half-lives. In both Figs. 6 and 7 the ^{208}Tl and ^{212}Bi curves follow the ^{212}Pb response curve closely due to the relatively large ratio of the ^{212}Pb to the ^{212}Bi and ^{208}Tl half-lives.

In Fig. 7 the effect of a 50% ^{212}Pb release can be seen. A more dramatic decline in the ^{208}Tl-^{212}Bi curve is noticeable because a larger quantity of ^{212}Pb has been removed. Again, the ^{208}Tl and ^{212}Bi curves follow the slowly ascending ^{212}Pb curve closely.

Finally, in Fig. 8 the effect of ^{212}Bi release is demonstrated. Both ^{208}Tl and ^{212}Bi lie on the same curve due to the short half-life of ^{208}Tl compared with that of ^{212}Bi and to the time interval under study. Equilibrium is observed within eight hours after the forcing function is removed because of the relatively short half-life of ^{212}Bi compared to the time interval. A curve representing ^{208}Tl response is not presented since it would appear merely as a step change due to its short half-life.

Two conclusions may be drawn from an analysis of Figs. 5 through 8. First, the magnitude of the depression of the ^{208}Tl curve is proportional to the quantity of the decay chain species released during the heating period; and, second, the shape of the ^{208}Tl response curve is a function of the species being released. Both of these phenomena may now be applied in the analysis of the experimental data to determine the type and to estimate the quantity of the species being released.

4.2 Experimental Results

Preliminary experiments were conducted in the conversion furnace at heating rates of 40 and 20 °C/min to determine the highest rate of heating the resin particles could tolerate. Figures 9 and 10 are photographs at 20X magnification of the resin sample after heating to 600°C at a rate of 40 and 20 °C/min, respectively. As can be seen from the photographs, the resin appears to be composed of a mixture of dull and shiny spheres and a number of irregularly-shaped particles. The dull surfaces correspond to the interior of those beads that cracked during the heating period, while

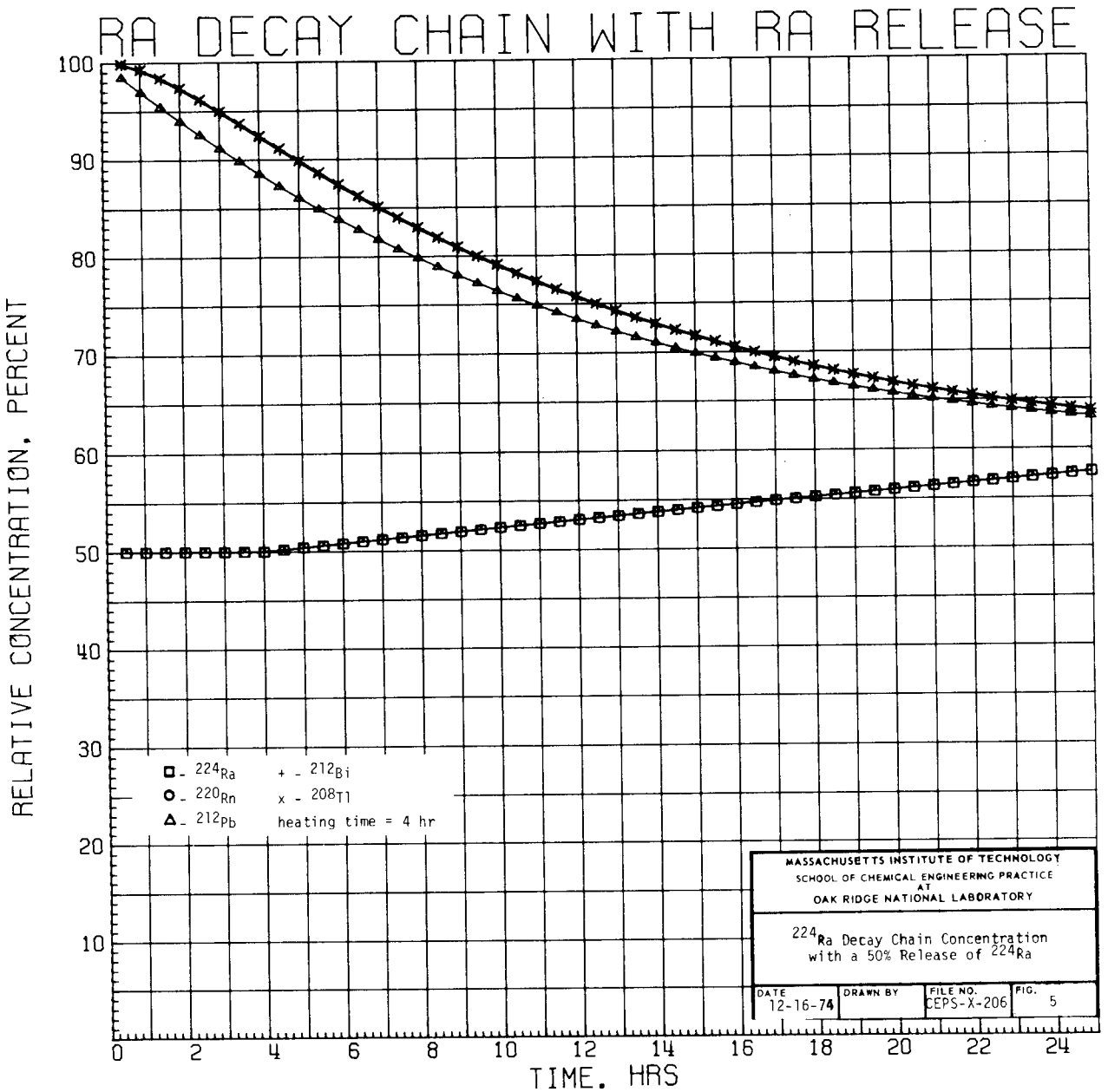
RA DECAY CHAIN WITH RA RELEASE
RELATIVE CONCENTRATION, PERCENT
TIME, HRS
100
90
80
70
60
50
40
30
20
10
0
2
4
6
8
10
12
14
16
18
20
22
24
□ - 224Ra
+ - 212Bi
O - 220Rn
x - 208Tl
Δ - 212Pb
heating time = 4 hr
MASSACHUSETTS INSTITUTE OF TECHNOLOGY
SCHOOL OF CHEMICAL ENGINEERING PRACTICE
AT
OAK RIDGE NATIONAL LABORATORY
224Ra Decay Chain Concentration
with a 50% Release of 224Ra
DATE
12-16-74
DRAWN BY
FILE NO.
CEPS-X-206
FIG.
5

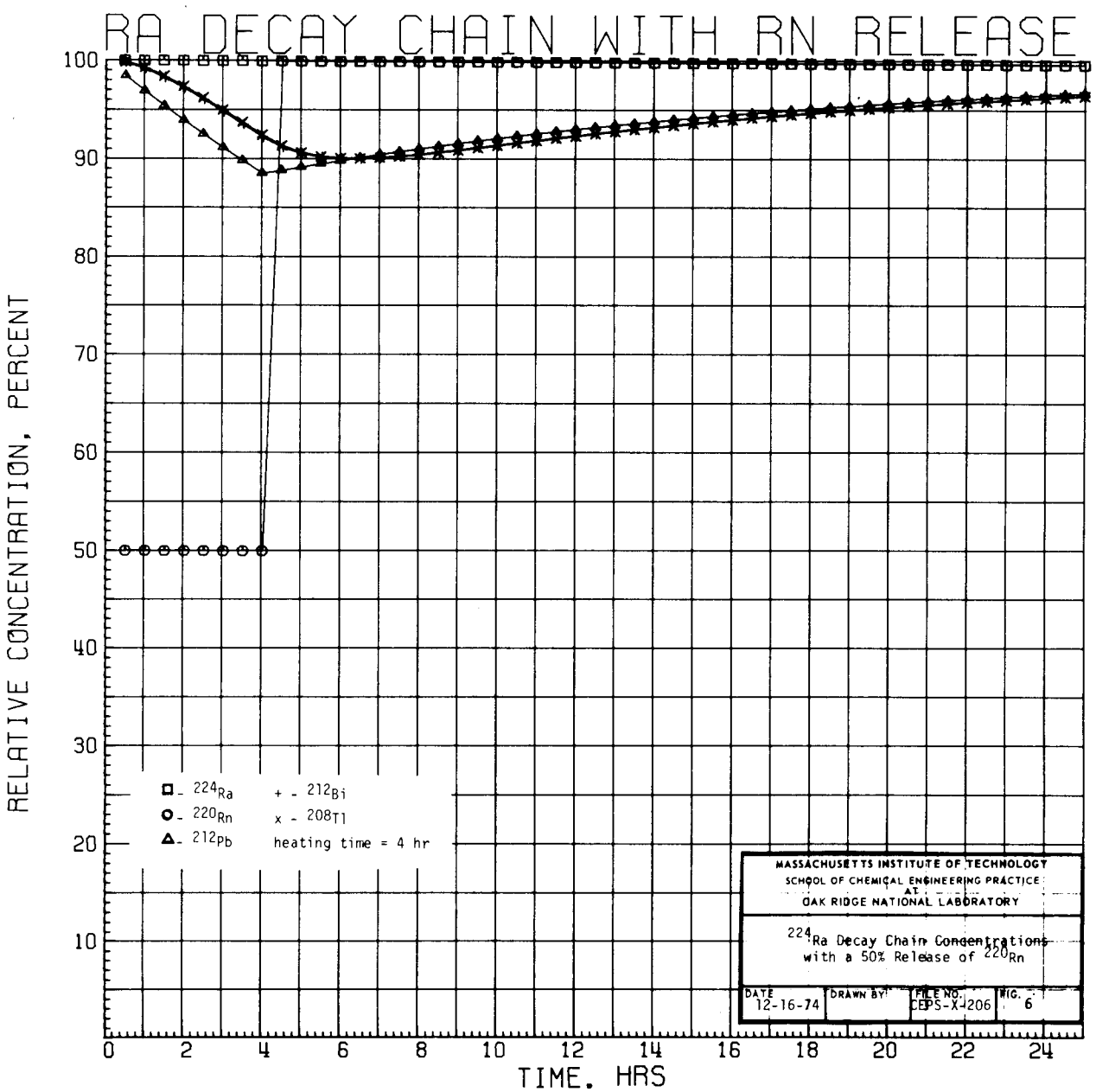
RA DECAY CHAIN WITH RN RELEASE
RELATIVE CONCENTRATION, PERCENT
100
90
80
70
60
50
40
30
20
10
0
2
4
6
8
10
12
14
16
18
20
22
24
TIME, HRS
□ - 224Ra
○ - 220Rn
△ - 212Pb
+ - 212Bi
x - 208Tl
heating time = 4 hr
MASSACHUSETTS INSTITUTE OF TECHNOLOGY
SCHOOL OF CHEMICAL ENGINEERING PRACTICE
AT
OAK RIDGE NATIONAL LABORATORY
224Ra Decay Chain Concentrations
with a 50% Release of 220Rn
DATE
12-16-74
DRAWN BY
FILE NO.
CEPS-X-206
FIG.
6

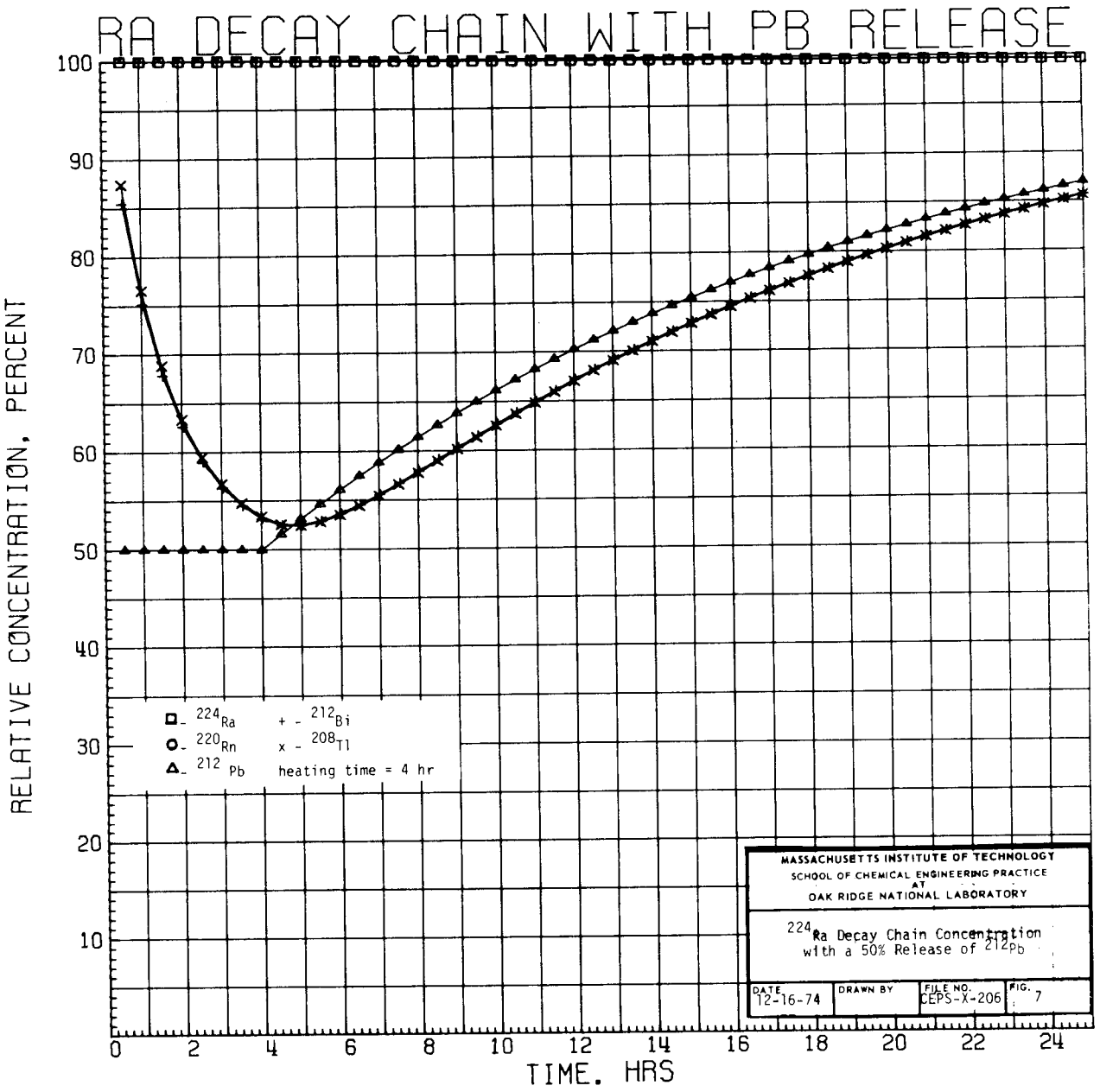
RA DECAY CHAIN WITH PB RELEASE
RELATIVE CONCENTRATION, PERCENT
TIME, HRS
100
90
80
70
60
50
40
30
20
10
0
2
4
6
8
10
12
14
16
18
20
22
24
□ - 224Ra
+ - 212Bi
O - 220Rn
x - 208Tl
Δ - 212 Pb
heating time = 4 hr
MASSACHUSETTS INSTITUTE OF TECHNOLOGY
SCHOOL OF CHEMICAL ENGINEERING PRACTICE
AT
OAK RIDGE NATIONAL LABORATORY
224Ra Decay Chain Concentration
with a 50% Release of 212Pb
DATE 12-16-74
DRAWN BY
FILE NO. CEPS-X-206
FIG. 7

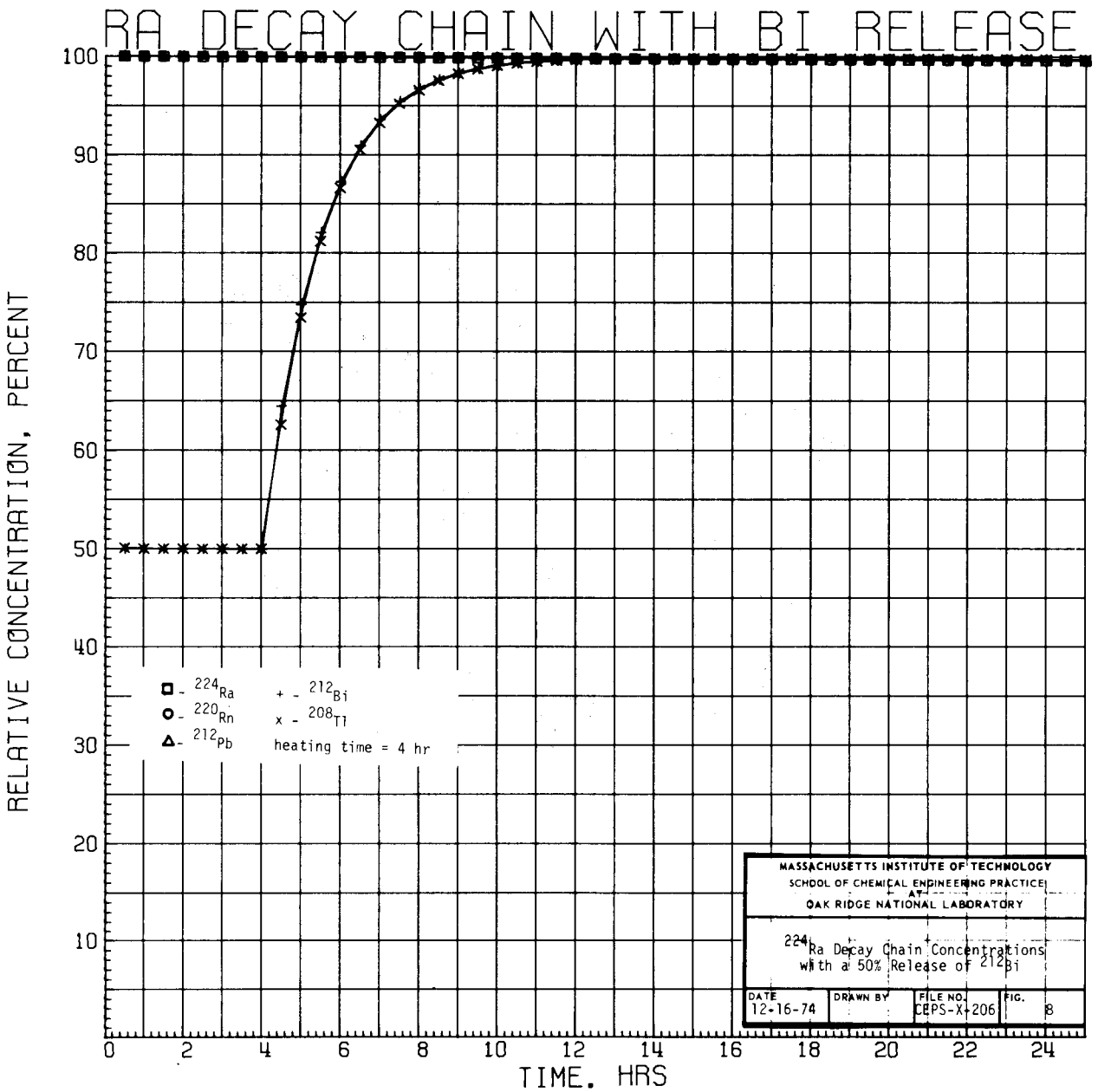
RA DECAY CHAIN WITH BI RELEASE
RELATIVE CONCENTRATION, PERCENT
TIME, HRS
100
90
80
70
60
50
40
30
20
10
0
2
4
6
8
10
12
14
16
18
20
22
24
□ - 224Ra
+ - 212Bi
○ - 220Rn
x - 208Tl
△ - 212Pb
heating time = 4 hr
MASSACHUSETTS INSTITUTE OF TECHNOLOGY
SCHOOL OF CHEMICAL ENGINEERING PRACTICE
AT
OAK RIDGE NATIONAL LABORATORY
224Ra Decay Chain Concentrations
with a 50% Release of 212Bi
DATE
12-16-74
DRAWN BY
FILE NO.
CEPS-X-206
FIG.
8

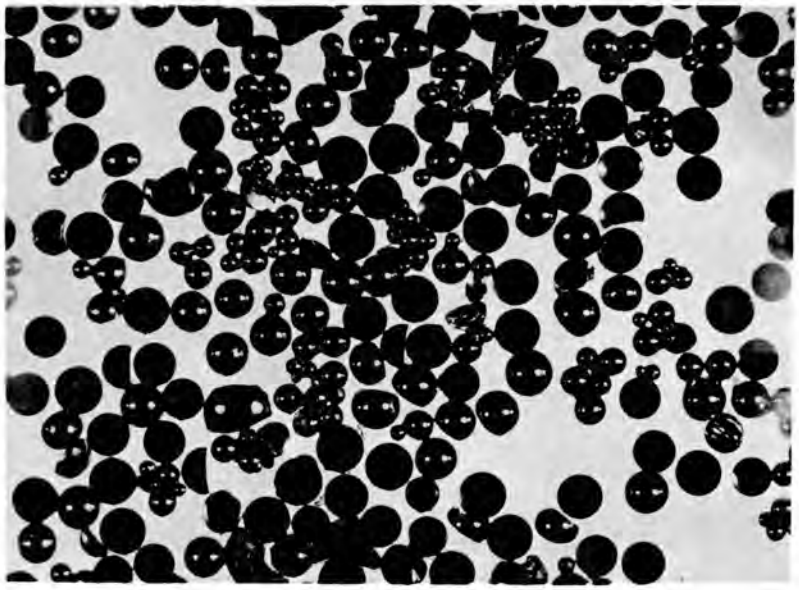

MASSACHUSETTS INSTITUTE OF TECHNOLOGY
SCHOOL OF CHEMICAL ENGINEERING PRACTICE
AT
OAK RIDGE NATIONAL LABORATORY

UNSORTED RESIN HEATED TO 600°C at 40°/min

DATE	DRAWN BY	FILE NO.	FIG.
12-16-74		CEPS-X-206	9

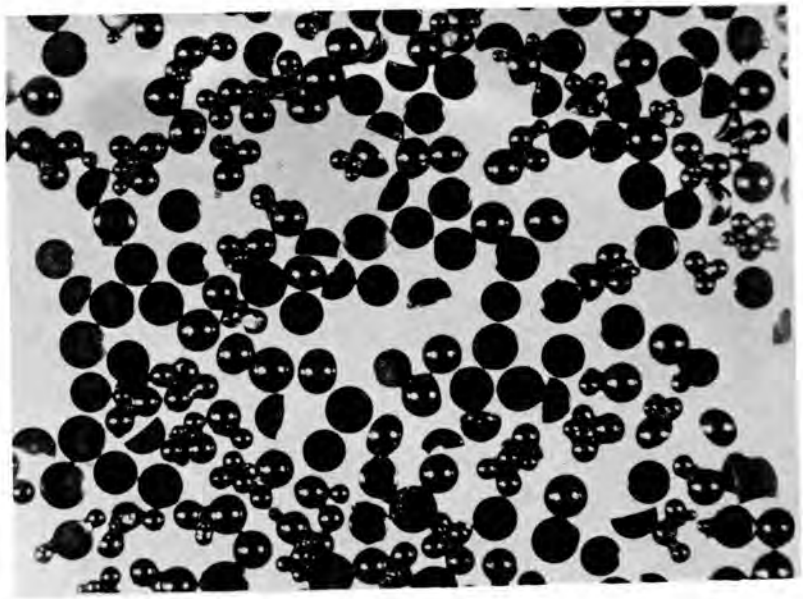

MASSACHUSETTS INSTITUTE OF TECHNOLOGY
SCHOOL OF CHEMICAL ENGINEERING PRACTICE
AT
OAK RIDGE NATIONAL LABORATORY

UNSORTED RESIN HEATED TO 600°C AT 20°/min

DATE	DRAWN BY	FILE NO.	FIG.
12-16-74		CEPS-X-206	10

the shiny surfaces are those that remained intact throughout the process. Cracking occurs because the particle surface cannot expand as rapidly as volatiles are evolved in the particles, causing an internal pressure buildup. A heating rate of 20 or 40°C/min appears to have little effect on the fraction of cracked beads (see Figs. 9 and 10).

Before a lower heating rate was tried, the resin was shape-separated to eliminate the irregular and conglomerated particles seen in Figs. 9 and 10. Of a batch of 184 gm of resin, 147 gm were separated as the spherical fraction and 37 gm were set aside as the irregular fraction. Figure 11 shows the shape-separated unheated resin; some irregularities still remain, but the particle agglomerations present prior to the separation have been removed. The shape-separated resin after heating to 600°C at 10°C/min is shown in Fig. 12. The uniformity of the resin particles is evident as is the low incidence of cracking at this slower heating rate. As a result of these preliminary experiments, 10°C/min was selected as the heating rate for all subsequent experimentation.

The background count of the sample containers prior to their use in an experiment appear in Table 2. The gamma count per second was obtained using the efficiencies obtained from other data (see sample calculation in Appendix 9.4). Background can be safely neglected after inspection of Table 2, since the range of thallium activity encountered in this investigation was approximately 600 to 1500 gamma counts per second.

Table 2. Background Count of Sample Containers

Sample Container No.	Run No.	$GPS_{583\ keV}$	$GPS_{2615\ keV}$
1	199	-	-
2	200	3.2	2.9
3	201	1.8	1.8
4	202	1.9	3.1
5	203	1.5	4.4
6	204	2.0	2.2
7	205	2.5	5.3
8	206	1.2	4.4

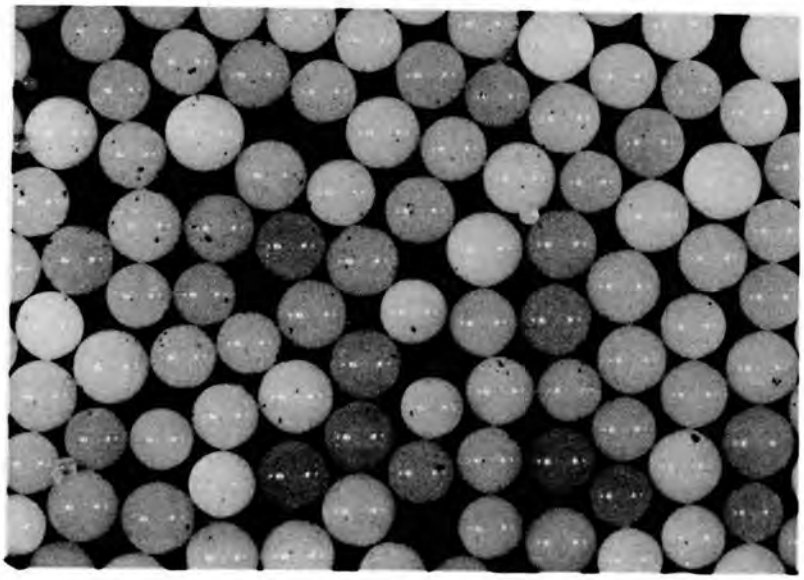

MASSACHUSETTS INSTITUTE OF TECHNOLOGY
SCHOOL OF CHEMICAL ENGINEERING PRACTICE
AT
OAK RIDGE NATIONAL LABORATORY

UNHEATED SHAPE-SEPARATED RESIN

DATE	DRAWN BY	FILE NO.	FIG.
12-12-74		CEPS-X-206	11

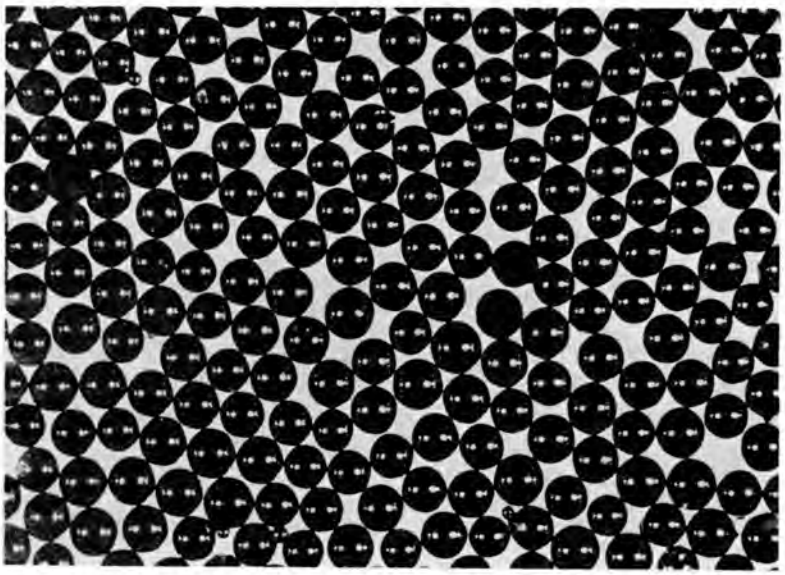

MASSACHUSETTS INSTITUTE OF TECHNOLOGY
SCHOOL OF CHEMICAL ENGINEERING PRACTICE
AT
OAK RIDGE NATIONAL LABORATORY

SHAPE-SEPARATED RESIN HEATED
TO 600°C AT 10°/MIN

DATE	DRAWN BY	FILE NO.	FIG.
12-16-74		CEPS-X-206	12

Figures 13 through 16 are plots of experimental relative thallium activity for four runs in which the temperature of the furnace was raised to 400, 500, 600, and 700°C, respectively, and held at the respective temperature for four hours. The relative thallium activity obtained from a computer simulation assuming 100% removal of ^{220}Rn is also shown on each of these plots. The data obtained from the 800°C run are shown in Fig. 17 which includes the simulated relative thallium activity resulting from 100% ^{220}Rn loss and some ^{212}Pb and ^{212}Bi loss.

Comparison of the experimental results when the furnace temperature was raised to 1000°C and held for four hours, and the predicted ^{208}Tl activity when all species below and including ^{220}Rn are completely removed is found in Fig. 18. The relative ^{208}Tl activity monitored from samples that had undergone simulation of the actual carbonization and conversion steps (i.e., slow heating to 600°C at 2°C/min followed by rapid heating to 1700°C at 90°C/min) is shown in Figs. 19 and 20.

4.3 Diffusion Modeling

Decay species in secular equilibrium in the ^{232}Th decay chain have formation and decay rates equal to the ^{232}Th decay rate of 3.7×10^{-25} moles/bead-sec (calculated in Appendix 9.4) or approximately one decay per bead every five seconds. A model describing a pore diffusion flux of less than one atom per second is, however, statistically meaningless, and therefore inapplicable. Moreover, the diffusivity of atoms through pores in the bead may not be a typical one. Beta and alpha decays occur continually and are known to propel atoms (6) thereby increasing effective diffusivity.

5. DISCUSSION

5.1 Comparison of Thorium and Uranium Loaded Resins

The resin used in the HTGR fuel refabrication process will be loaded with uranium rather than thorium. The ratio of ^{232}U to ^{232}Th activity, obtained as the quotient of their respective decay rates, is 2.9×10^{5}. Safety, therefore, was the primary reason for using a thorium-loaded resin. As can be seen from Fig. 1, the decay chains of ^{232}Th and ^{232}U are identical after ^{228}Th and fortunately it is that part of the chain from ^{224}Ra to ^{208}Tl that is directly involved in the experiments.

Since one objective was to measure ^{224}Ra losses from the resin, some concern existed over the possible interference of ^{228}Ra, which occurs in the ^{232}Th chain but not in the ^{232}U chain. Luckily, any change in the ^{228}Ra concentration occurring during the refabrication step would not begin to affect the measured ^{208}Tl activity for many years because of the long half-life of ^{228}Th (1.9 yr) relative to those of ^{224}Ra and ^{220}Rn.

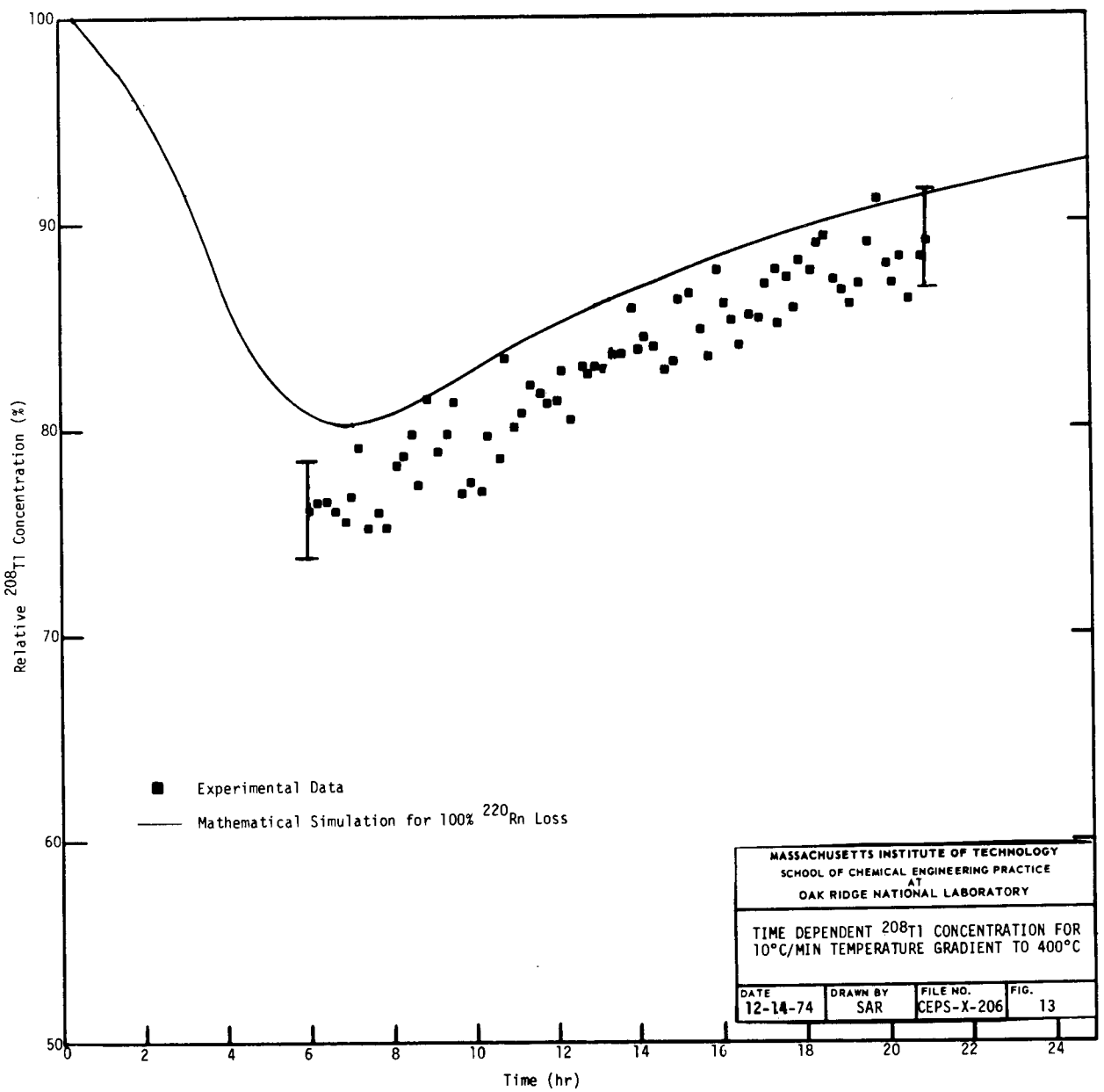
100
90
80
70
60
50
Relative 208Tl Concentration (%)
0
2
4
6
8
10
12
14
16
18
20
22
24
Time (hr)
Experimental Data
Mathematical Simulation for 100% 220Rn Loss
MASSACHUSETTS INSTITUTE OF TECHNOLOGY
SCHOOL OF CHEMICAL ENGINEERING PRACTICE
AT
OAK RIDGE NATIONAL LABORATORY
TIME DEPENDENT 208Tl CONCENTRATION FOR
10°C/MIN TEMPERATURE GRADIENT TO 400°C
DATE
12-14-74
DRAWN BY
SAR
FILE NO.
CEPS-X-206
FIG.
13

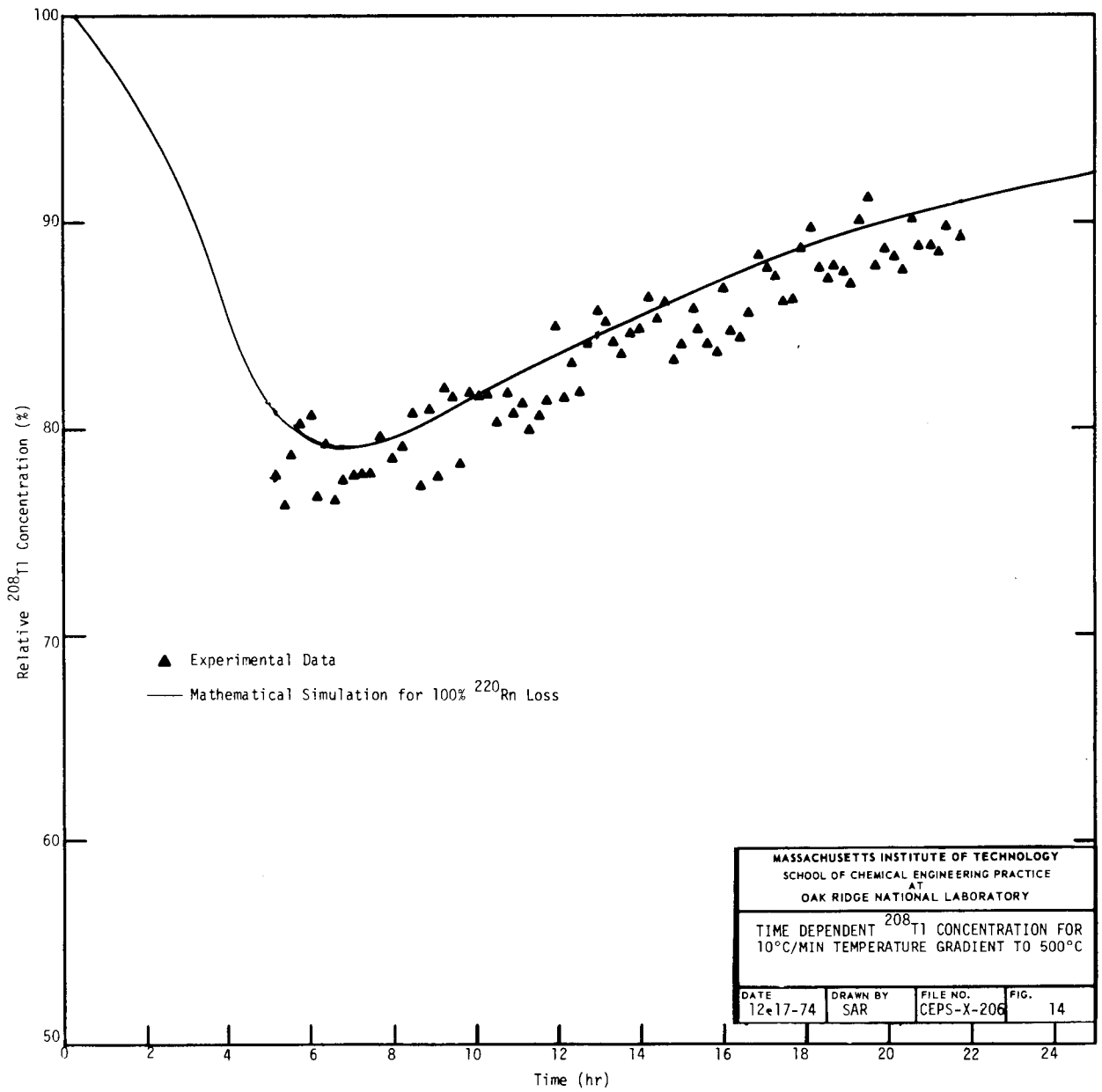
100
90
80
70
60
50
Relative ^{208}Tl Concentration (%)
0
2
4
6
8
10
12
14
16
18
20
22
24
Time (hr)
Experimental Data
Mathematical Simulation for 100% ^{220}Rn Loss
MASSACHUSETTS INSTITUTE OF TECHNOLOGY
SCHOOL OF CHEMICAL ENGINEERING PRACTICE
AT
OAK RIDGE NATIONAL LABORATORY
TIME DEPENDENT ^{208}Tl CONCENTRATION FOR
10°C/MIN TEMPERATURE GRADIENT TO 500°C
DATE
12-17-74
DRAWN BY
SAR
FILE NO.
CEPS-X-206
FIG.
14

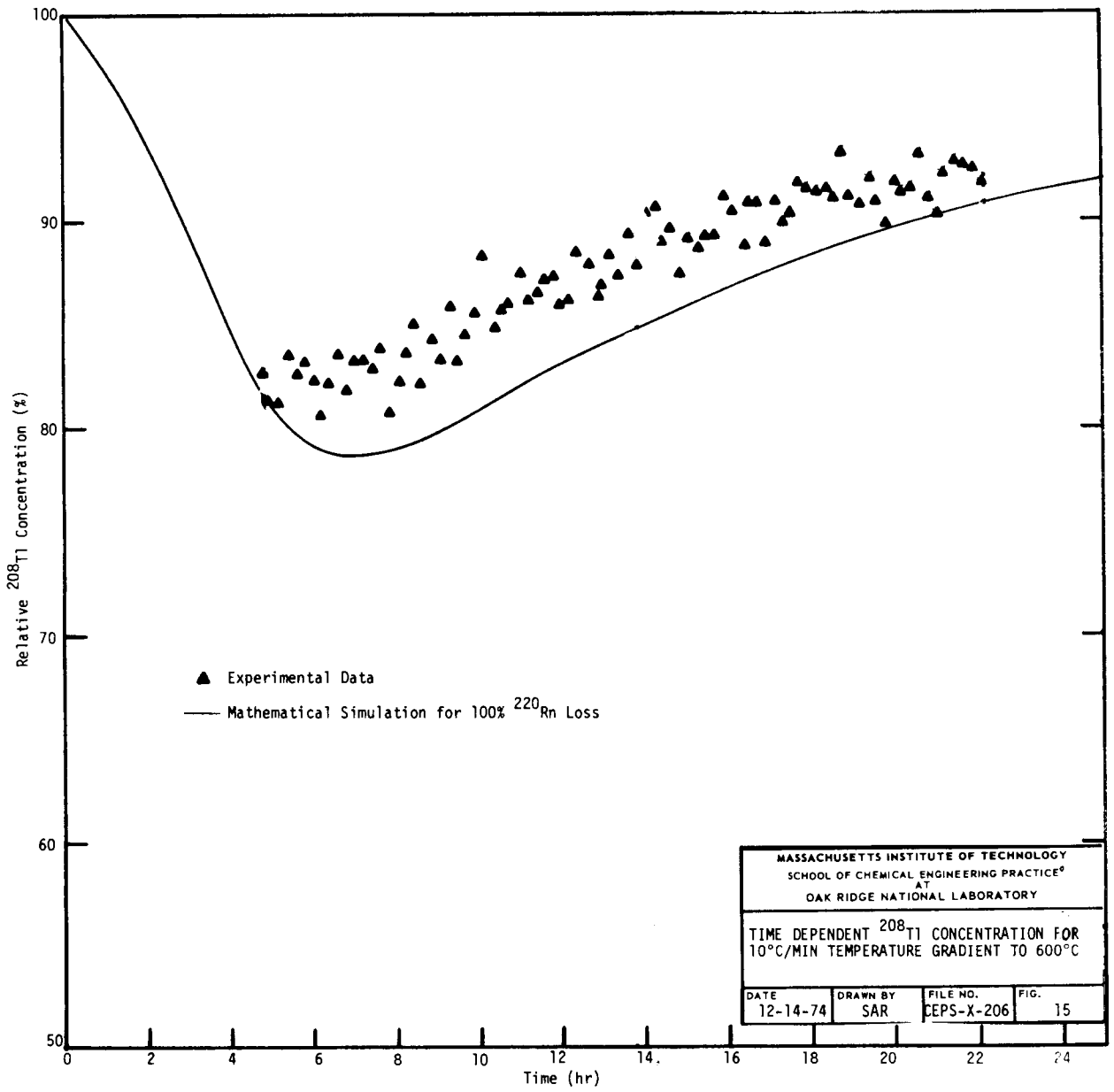
100
90
80
70
60
50
Relative 208Tl Concentration (%)
0
2
4
6
8
10
12
14
16
18
20
22
24
Time (hr)
Experimental Data
Mathematical Simulation for 100% 220Rn Loss
MASSACHUSETTS INSTITUTE OF TECHNOLOGY
SCHOOL OF CHEMICAL ENGINEERING PRACTICE
AT
OAK RIDGE NATIONAL LABORATORY
TIME DEPENDENT 208Tl CONCENTRATION FOR
10°C/MIN TEMPERATURE GRADIENT TO 600°C
DATE 12-14-74
DRAWN BY SAR
FILE NO. CEPS-X-206
FIG. 15

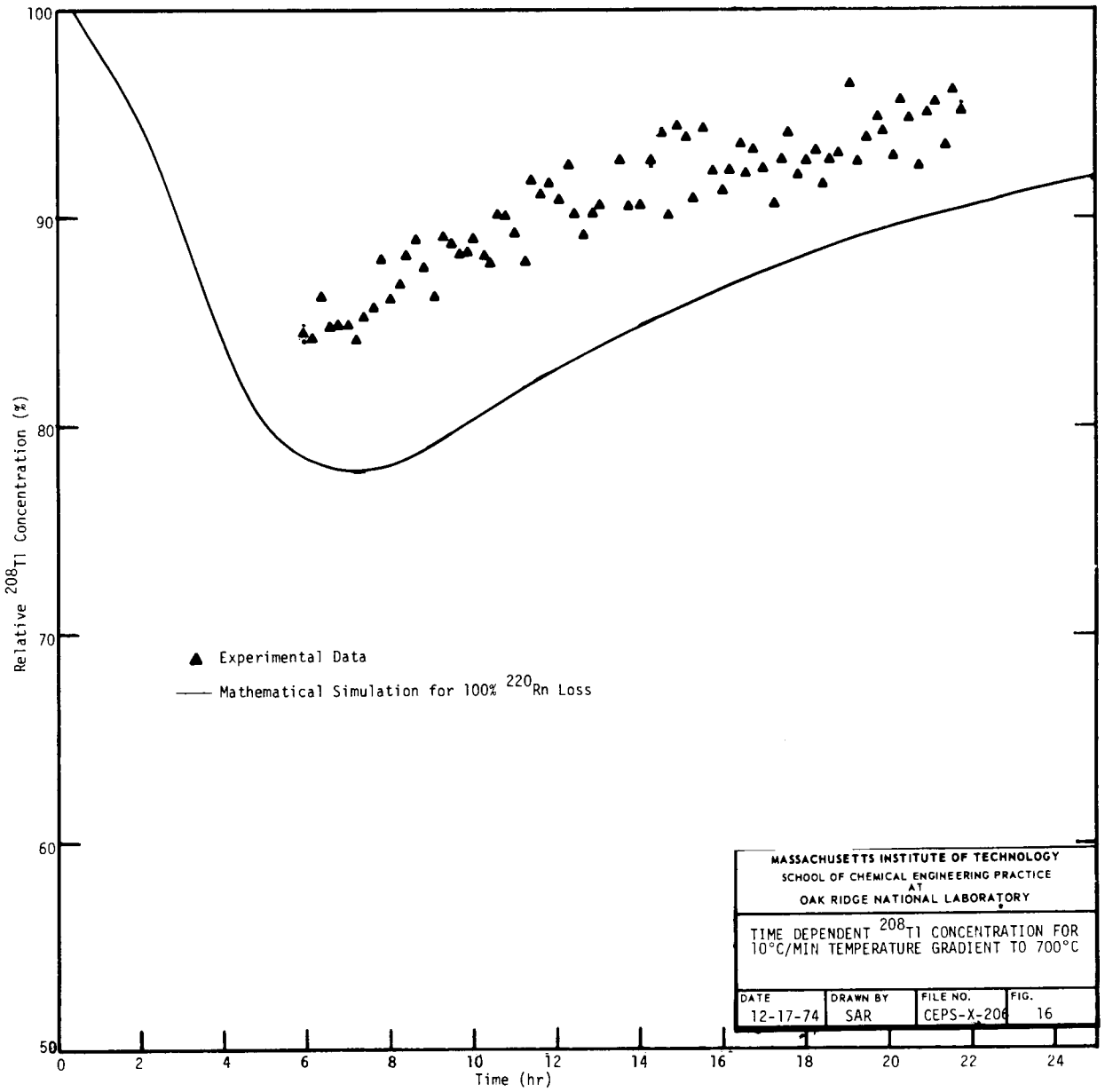
100
90
80
70
60
50
Relative 208Tl Concentration (%)
0
2
4
6
8
10
12
14
16
18
20
22
24
Time (hr)
Experimental Data
Mathematical Simulation for 100% 220Rn Loss
MASSACHUSETTS INSTITUTE OF TECHNOLOGY
SCHOOL OF CHEMICAL ENGINEERING PRACTICE
AT
OAK RIDGE NATIONAL LABORATORY
TIME DEPENDENT 208Tl CONCENTRATION FOR
10°C/MIN TEMPERATURE GRADIENT TO 700°C
DATE
12-17-74
DRAWN BY
SAR
FILE NO.
CEPS-X-206
FIG.
16

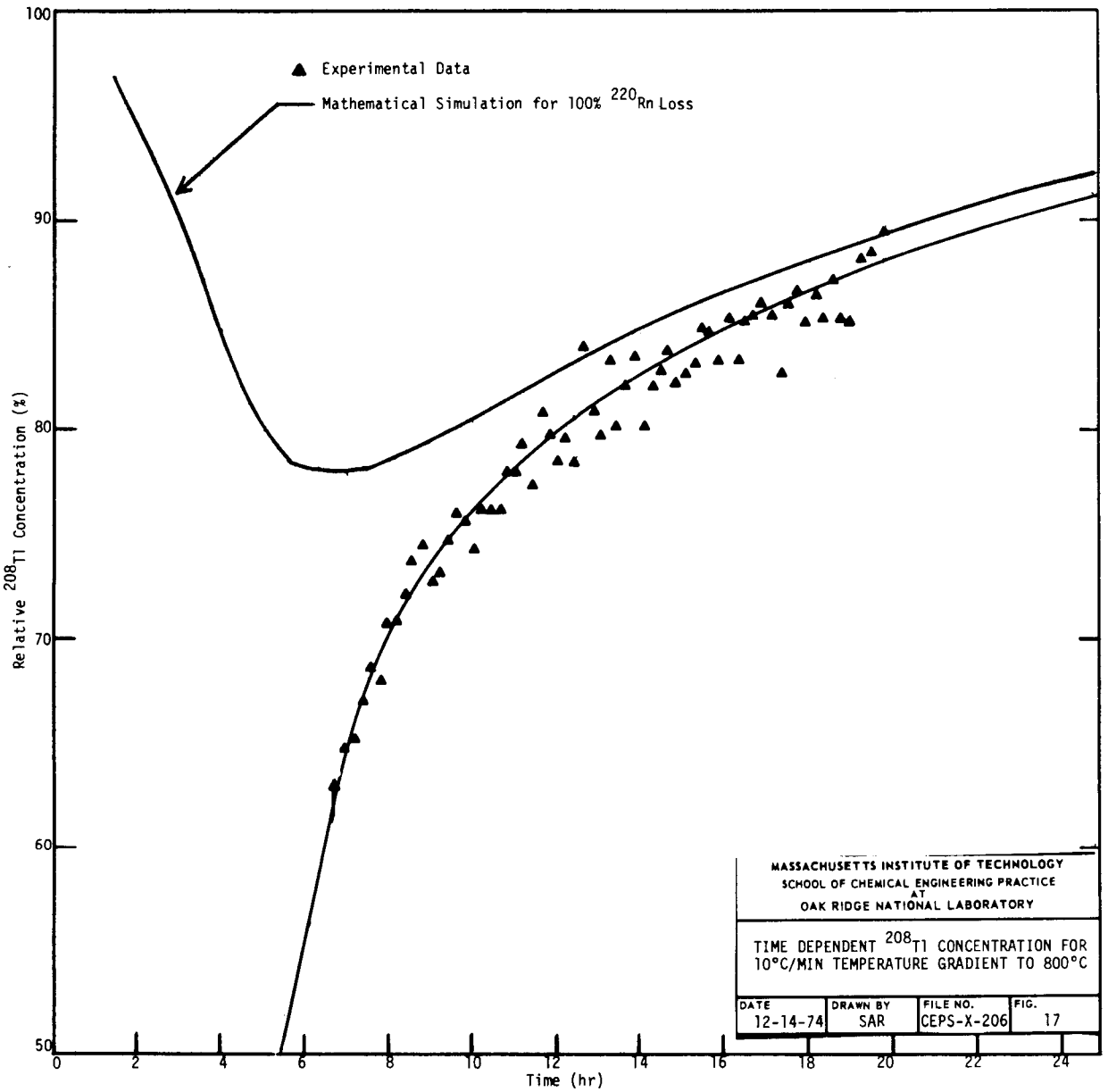
Experimental Data
Mathematical Simulation for 100% 220Rn Loss
Relative 208Tl Concentration (%)
Time (hr)
100
90
80
70
60
50
0
2
4
6
8
10
12
14
16
18
20
22
24
MASSACHUSETTS INSTITUTE OF TECHNOLOGY
SCHOOL OF CHEMICAL ENGINEERING PRACTICE
AT
OAK RIDGE NATIONAL LABORATORY
TIME DEPENDENT 208Tl CONCENTRATION FOR
10°C/MIN TEMPERATURE GRADIENT TO 800°C
DATE
12-14-74
DRAWN BY
SAR
FILE NO.
CEPS-X-206
FIG.
17

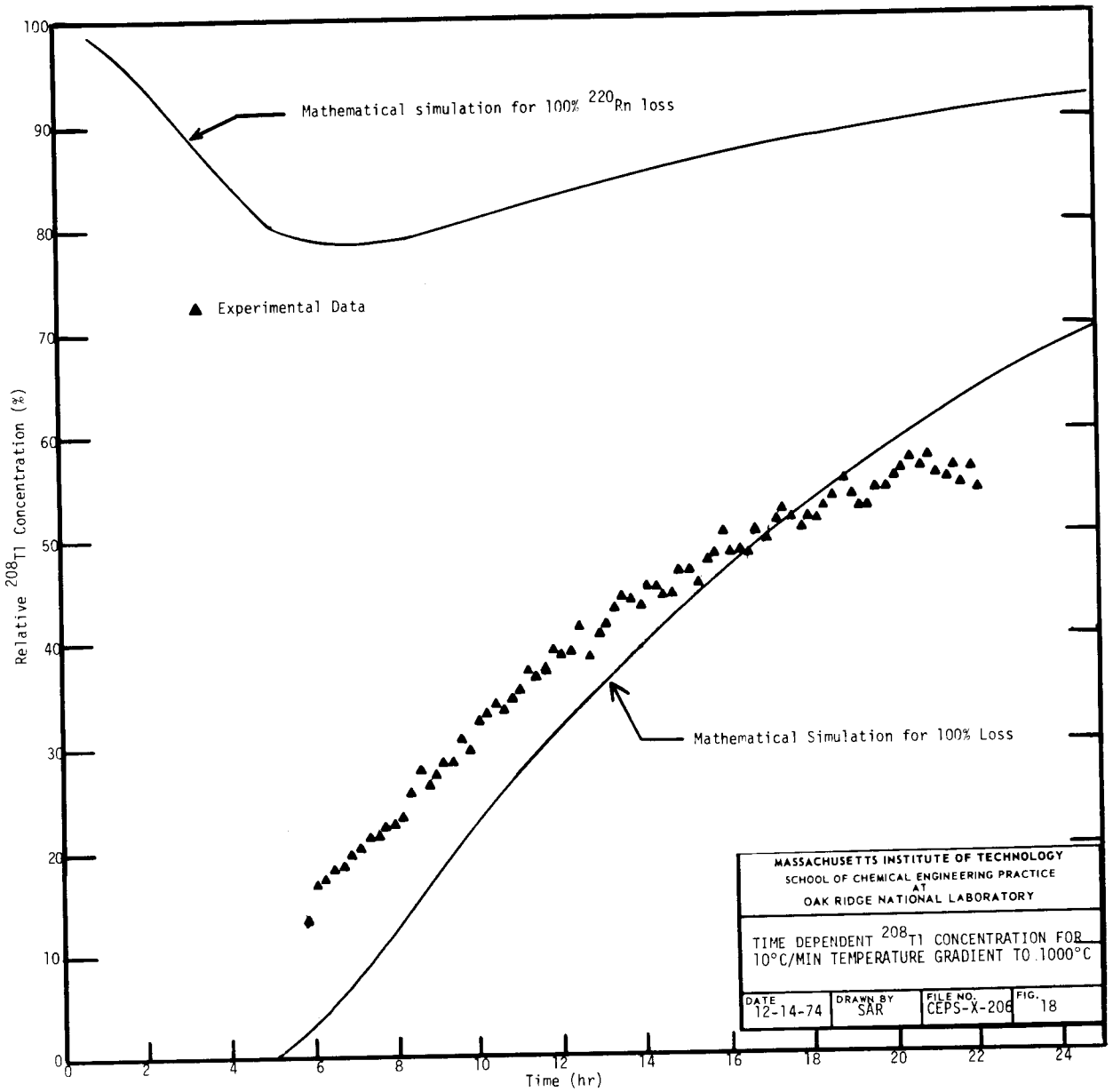
Mathematical simulation for 100% 220Rn loss
Experimental Data
Mathematical Simulation for 100% Loss
Relative 208Tl Concentration (%)
Time (hr)
0
10
20
30
40
50
60
70
80
90
100
0
2
4
6
8
10
12
14
16
18
20
22
24
MASSACHUSETTS INSTITUTE OF TECHNOLOGY
SCHOOL OF CHEMICAL ENGINEERING PRACTICE
AT
OAK RIDGE NATIONAL LABORATORY
TIME DEPENDENT 208Tl CONCENTRATION FOR
10°C/MIN TEMPERATURE GRADIENT TO 1000°C
DATE 12-14-74
DRAWN BY SAR
FILE NO. CEPS-X-206
FIG. 18

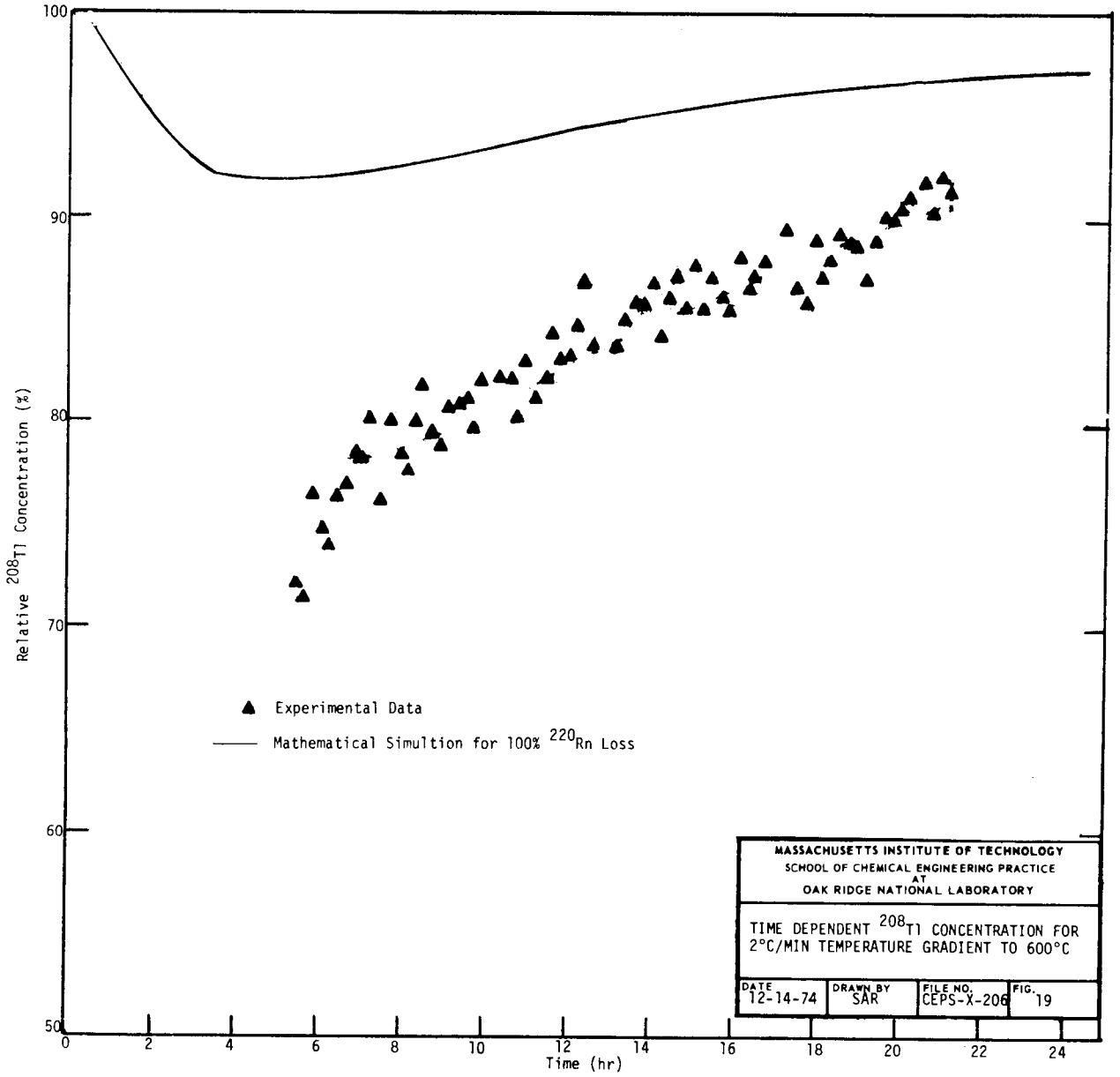
100
90
80
70
60
50
Relative ^{208}Tl Concentration (%)
0
2
4
6
8
10
12
14
16
18
20
22
24
Time (hr)
Experimental Data
Mathematical Simultion for 100% ^{220}Rn Loss
MASSACHUSETTS INSTITUTE OF TECHNOLOGY
SCHOOL OF CHEMICAL ENGINEERING PRACTICE
AT
OAK RIDGE NATIONAL LABORATORY
TIME DEPENDENT ^{208}Tl CONCENTRATION FOR
2°C/MIN TEMPERATURE GRADIENT TO 600°C
DATE 12-14-74
DRAWN BY SAR
FILE NO. CEPS-X-206
FIG. 19

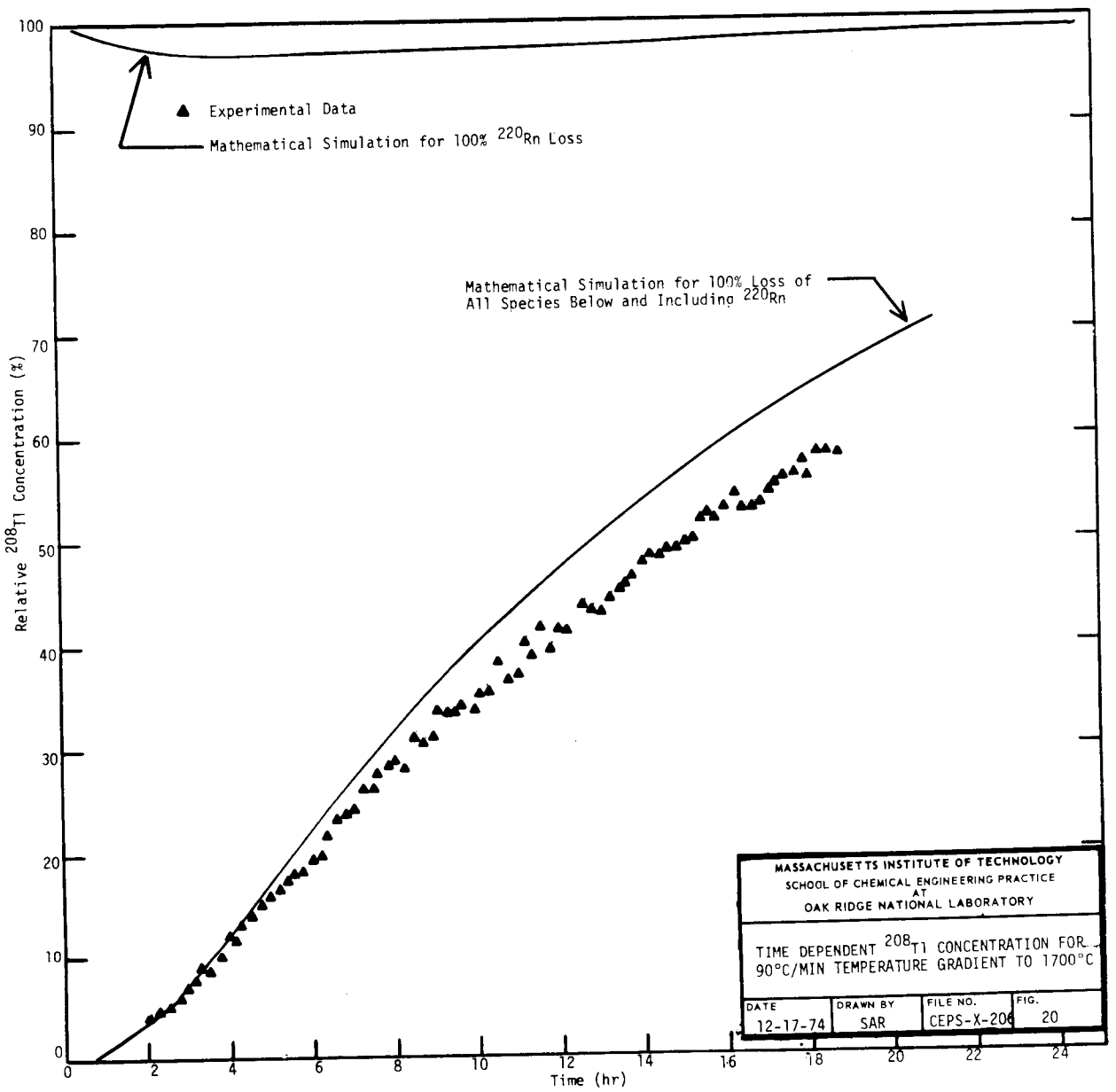
Experimental Data
Mathematical Simulation for 100% 220Rn Loss
Mathematical Simulation for 100% Loss of All Species Below and Including 220Rn
Relative 208Tl Concentration (%)
Time (hr)
0
10
20
30
40
50
60
70
80
90
100
0
2
4
6
8
10
12
14
16
18
20
22
24
MASSACHUSETTS INSTITUTE OF TECHNOLOGY
SCHOOL OF CHEMICAL ENGINEERING PRACTICE
AT
OAK RIDGE NATIONAL LABORATORY
TIME DEPENDENT 208Tl CONCENTRATION FOR 90°C/MIN TEMPERATURE GRADIENT TO 1700°C
DATE 12-17-74
DRAWN BY SAR
FILE NO. CEPS-X-206
FIG. 20

One additional point should be clarified concerning the simulation of uranium-loaded resin with thorium-loaded resin. Daughter nuclide concentrations in the HTGR resin will be higher than those encountered in the experimental resin because of the short half-life of ^{232}U relative to ^{232}Th. Tables 3 and 4 show the calculated equilibrium concentrations of ^{232}Th and ^{232}U and their daughter nuclide concentrations. The question might still arise, however, that some diffusion limitation might exist at the higher ^{232}U concentrations that would not be apparent at the lower ^{232}Th ones. This possibility can be neglected for two reasons. First, inspection of Tables 3 and 4 indicates that while ^{232}U daughter concentrations are higher than those of ^{232}Th, the absolute concentrations are still very small, well below the region where mass transfer limitations would be expected to be controlling. Secondly, the effective diffusivity of the daughters within the bead can be augmented by their α and β emissions (6). The emission of α and β particles and their diffusion from the pore are random events, however, the escaping α and β particles add to the overall diffusion. Radioactive atoms are propelled by emission of alpha and beta particles; thus, the diffusivity may be controlled by rates of α and β decay rather than by Knudsen diffusion within the beads' pores.

5.2 Comparison of Theoretical and Experimental Results

The data presented in Figs. 13-20 are expressed as relative ^{208}Tl concentration versus time in hours. Relative ^{208}Tl activity was obtained by dividing each individual activity reading by the average ^{208}Tl activity of the same sample at secular equilibrium. For use as reference samples, the heated beads from each experimental run were allowed to reattain secular equilibrium which requires approximately 100 hr. Unheated samples were not used as a reference for two reasons. First, using the same heated beads for both the experimental and reference samples reduced experimental error; since the same sample was used for each, both sample containers were filled to precisely the same point, eliminating errors in gamma detection due to geometric factors. Secondly, the different densities of heated and unheated samples, 2 vs 1 g/cc, respectively, resulted in different amounts of self-absorption of gamma rays or attenuation.

Gamma attenuation, Q, is calculated as:

$$Q = e^{-N\rho x} \tag{11}$$

where:

N = mass attenuation coefficient

ρ = density

x = distance through sample traversed by gamma rays

Table 3. Equilibrium Concentration of ^{232}U and Daughter Nuclides

Basis: Resin beads 32% by weight U; U 1500 ppm by weight ^{232}U; mass of bead = 1.7×10^{-4} g/bead

Species	Half-Life (4)	Equilibrium Concentration (moles/bead)
^{232}U	72 yr	3.50×10^{-10}
^{228}Th	1.9 yr	9.24×10^{-12}
^{224}Ra	3.64 days	4.85×10^{-14}
^{220}Rn	54.5 sec	8.40×10^{-18}
^{216}Po	0.158 sec	2.44×10^{-20}
^{212}Pb	10.6 hr	5.88×10^{-15}
^{212}Bi	60.6 min	5.60×10^{-16}
^{208}Tl	3.1 min	1.03×10^{-17}

Table 4. Concentrations of Members of ^{232}Th Decay Chain

Basis: Resin beads 32% by weight ^{232}Th; mass of bead = 1.7×10^{-4} g/bead

Species	Half-Life (4)	Equilibrium Concentration (moles/bead)
^{232}Th	1.39×10^{10} yr	2.34×10^{-7}
^{228}Ra	5.75 yr	9.68×10^{-17}
^{228}Ac	6.13 hr	1.18×10^{-20}
^{228}Th	1.9 yr	3.20×10^{-17}
^{224}Ra	3.64 days	1.68×10^{-19}
^{220}Rn	54.5 sec	2.91×10^{-23}
^{216}Po	0.158 sec	8.43×10^{-26}
^{212}Pb	10.6 hr	2.04×10^{-20}
^{212}Bi	60.6 min	1.94×10^{-21}
^{208}Th	3.1 min	3.57×10^{-23}

Note: The thallium concentration above is based on a 36/64% split of ^{212}Bi to ^{208}Tl and ^{212}Po, respectively (see Fig. 1).

When several species are present, e.g., ^{232}Th, C, H, O, and N as in the resin used, the total attenuation, Q_t, is determined by multiplying the attenuations due to each species:

$$Q_t = e^{-(\sum_i N_i \rho_i x)} \tag{12}$$

Table 5 presents the unheated reference and heated reference sample activities along with the observed difference. A sample calculation of the attenuation can be found in Appendix 9.4. The agreement between average observed difference and that calculated for self shielding suggests that the difference in activity for the two types of samples can be explained by attenuation or shielding effects.

Table 5. Comparison of Calculated and Observed Attenuation Differences in Heated and Unheated Steady-State Samples

Temperature (°C)	Heated Sample Activity GPS	Unheated Sample Activity GPS	Observed Difference (%)
400	1440	1533	6.1
500	1504	1533	1.9
600	1475	1533	3.8
700	1502	1533	2.0
800	1438	1533	6.2
Average	1472	1533	4.0

The analysis of the experimental data was carried out by comparing the data (obtained by monitoring the relative ^{208}Tl activity with time) to computer generated ^{208}Tl activity simulations. These graphical comparisons can be found in Sect. 4.2. It has been shown in Sect. 4.1 that the depth of the ^{208}Tl depression and the shape of the response curve are functions of the quantity and identity of the decay chain species released. Therefore, by applying combinations of forcing functions as described in Sect. 2.4.2, simulation curves have been developed which fit the data. Figure 13 represents data obtained at 400°C, which lie somewhat below, but have the same shape as the simulation produced by a release rate of ^{220}Rn equal to its equilibrium decay rate, i.e., 100% loss of ^{220}Rn. The error bars indicating the scatter in the data were calculated as shown in Appendix 9.4.6.

Figures 14, 15, and 16 represent the experimental data for runs conducted between 500 and 700°C and the comparison of these data with the simulation curve for a ^{220}Rn release rate equal to its equilibrium decay rate. The data at 500°C lie almost directly on the simulation curve; however, as the temperature increases to 600 and 700°C, the data points shift upward indicating a reduction in radon loss. No physical model has been proposed to explain this phenomena and one would expect the opposite - an increase in radon loss with increasing temperature. The trend cannot be explained as experimental error. In Table 6 a statistical summary of the average activity is recorded for each run after 74 hr. The experimental data from which this table was derived appears in Appendix 9.2. The value of 74 hr was chosen since the ^{208}Tl response curve follows the decay constant of the longest half-life in the chain after Rn, which is the 10.6 hr half-life of lead. Approximately seven half-lives or 74 hr are required for ^{208}Tl to return to secular equilibrium. An error analysis was performed using the statistical average of emission rates (obtained after 74 hr) for the reference sample activity. In no case was the error greater than 2.25% at 95% confidence. The average error was about 1.4%. This indicates that errors in experimental technique cannot justifiably explain the observed experimental results in Figs. 13 through 18.

Table 6. Error Associated with Averaging Equilibrium Samples

Run No.	Temperature (°C)	Average Equilibrium Activity CPS	σ	% Error (at 95% Confidence Limits)
199	800	1438	15.7	0.80
200	400	1440	20.6	1.18
201	600	1475	21.2	1.69
202	500	1504	28.7	2.25
203	700	1502	5.66	1.68
204	1000	1510	6.55	0.73

Another source of error is the measurement of the detector-to-sample-distance where an error of one millimeter can induce a 4% error in activity However, the reproducibility of the reference activities shown in Appendix 9.2 indicates that the distance was reproducible from trial to trial. From the range of values corresponding to each reference sample in Appendix 9.2, the maximum error associated with the detector-to-sample-distance is 0.5%.

Finally, a weighing error is associated with the activities which are reported per gram of ^{232}Th. If the weight fraction of thorium, 32%, in the bead before the carbonization step is known, and no losses of thorium

occur during the step, then the activities can be reported on this basis. However, the error associated with the top-loading Mettler balance used is only ±0.05 g/18 g or 0.3%.

The total contribution of the three sources of error is on the order of 2% and therefore does not explain the 8% discrepancy between the simulated and experimental curves shown in Figs. 13, 15, and 16.

The effect may be caused by structural changes in the bead as the temperature is increased thereby limiting gas release rates. Product beads from the 400°C run were observed to be significantly less dense than those from runs at 600 and 700°C, with a bead density of 1.49 g/cc for the lower temperature run and a 2 g/cc density for the two higher temperature runs. This effect is due to the incomplete carbonization of the beads at 400°C. Porosimetry data given in Appendix 9.3 indicate little change in the macropore structure with temperature. Though the resin beads are believed to have pore sizes on the order of 20-30 Å, no firm assessment can be made using the porosimetry results. A nitrogen adsorption investigation of pore sizes below 100 Å could be enlightening. Clearly replication of these data are necessary to confirm the observed deviations from the predicted value of ^{220}Rn loss. A method to check the above hypothesis is to precarbonize beads at 800°C and allow them to return to secular equilibrium. These beads may then be used for experiments at temperatures between 400 and 800°C in which the structural changes would presumably not occur.

Illustrated in Fig. 17 are data obtained at 800°C which fall well below the line corresponding to a 100% loss of ^{220}Rn. From the shape of the curve it is apparent that ^{212}Pb and ^{212}Bi are released at 800°C.

Figures 19 and 20 present data obtained from experimental simulations of the proposed uranium carbonization and conversion processes. For the data shown in Fig. 19, the thorium loaded resin was heated at a rate of 2°C/min to 600°C and held there for 15 min. The results shown in Fig. 20 were obtained when resin previously carbonized at 600°C (Fig. 15) was heated at 90°C/min to 1700°C and held at that temperature for half an hour. Analysis of the data shown in Figs. 18 and 20 indicates that significantly more ^{212}Pb and ^{212}Bi were released at temperatures between 1000 and 1700°C than was released at 800°C. Theoretical curves corresponding to 100% depletion of ^{220}Rn, ^{212}Pb, and ^{212}Bi during the heating period are also shown. Clearly, the experimental curves have significantly different shape and appear to level out before the predicted time. The data at 1000°C, however, did return to the secular equilibrium value after a period of 100 hr indicating that ^{224}Ra is not responsible for the losses. The data at 1700°C and 100 hr were, however, about 90% of, or about 9% below, the expected secular equilibrium value so the possibility exists that some ^{224}Ra may have been lost during the run. However, the poor fit of the simulation curves to the experimental data indicates that the actual release mechanism is more complex than the simple model used to describe the phenomena, but the comparison does allow an estimate of the quantity and type of species being released.

Figure 19 indicates the loss of ^{212}Bi since the curve has the proper shape and the data points fall significantly below 80% of the equilibrium

value associated with 100% loss of ^{220}Rn. Since this phenomenon was not observed previously at 600°C, as shown in Fig. 15, it is difficult to explain the losses of ^{212}Bi by abrasion of particles in the furnace. An abrasion mechanism must be discounted because any such effect would also cause the loss of ^{224}Ra from the beads. Such a loss of radium would be readily apparent in the experimental curves by a failure of the ^{208}Tl activity to return to equilibrium after 100 hr.

In summary, at temperatures between 400 and 700°C the predominant specie being released is ^{220}Rn as expected from its noble gas properties. At temperatures above 700°C, a significant fraction of ^{212}Pb and ^{212}Bi is also released, ^{212}Bi being released at a somewhat higher rate. Finally, at temperatures above 1000°C, the depletion of ^{220}Rn, ^{212}Pb, and ^{212}Bi species is virtually complete. During this study no evidence of significant ^{224}Ra removal has been observed. If radium had been removed, the ^{208}Tl activity curve would take almost a month to approach the equilibrium values. This effect could not be observed during any of the above experiments.

6. CONCLUSIONS

1. Concentrations of 10^{-16} to 10^{-26} moles/bead for decay species are too low to permit a statistically correct diffusion model analysis.

2. In experiments using furnace heatup rates of 10°C/min and ^{232}Th-loaded resin:

   a. Approximately 90-100% of the ^{220}Rn was lost as off-gas between 400 and 700°C as determined.

   b. The observed phenomenon of decreasing loss of relative ^{208}Tl activity with increasing temperature in the range of 400 to 700°C cannot be explained by experimental error.

   c. Approximately 100% of the ^{220}Rn, along with some ^{212}Pb and the ^{212}Bi was released at 800°C.

   d. Significantly more ^{220}Rn, ^{212}Pb, and ^{212}Bi were lost at 1000°C than at 800°C.

3. In experiments with furnace heatup rates of 2°C/min and ^{232}Th-loaded resin:

   a. Eighty to 100% of the ^{220}Rn and some ^{212}Bi are lost during a simulation of the carbonization step with a final temperature of 600°C.

   b. Some ^{224}Ra along with ^{212}Pb, ^{212}Bi, and ^{220}Rn was released during rapid heating to 1700°C.

4. No loss of ^{224}Ra was observed in any experiment with a furnace heatup rate of 10°C/min.

7. RECOMMENDATIONS

1. The 400-700°C data require replication. Previously carbonized beads should be used to eliminate the structural differences among beads at different temperatures. The 1000°C data should also be replicated since the low slope of its return to secular equilibrium is unexplained at this time.

2. If the refabrication facility design is based upon the data from this investigation, the design should allow sufficient capacity to handle a complete loss of radioactive gases.

3. The activity of the 1700°C sample should be rechecked. If it has not returned to equilibrium after 110 hr, the hypothesized loss of ^{224}Ra is substantiated.

4. The detector efficiency at 583 and 2615 keV should be determined for the sample holder geometry. Knowledge of this value would allow a secular equilibrium mass balance to be made based on ^{208}Tl activity which in turn would indicate the ^{220}Rn release rate at STP conditions.

5. Nitrogen sorption experiments should be carried out on pre-carbonized and carbonized beads to determine the extent of structural differences.

8. ACKNOWLEDGMENTS

The authors would like to thank F.F. Dyer and L.L. Fairchild for their indispensable guidance throughout the project and R.L. Beatty and C. Hamby, Jr., for their technical advice and assistance during the experimentation. We also thank our consultants, J.D. Jenkins, S.R. McNeany, and J.E. Rushton for their unfailing support and guidance.

9. APPENDIX

9.1 The Matrix Exponential Method for Solving Simultaneous Differential Equations

This section summarizes the matrix exponential method used to solve the equations describing the ^{224}Ra decay scheme. A more complete description of the history and background of the method is included in the MATEXP manual (1).

A set of nonhomogeneous equations which describe a decay scheme may be represented by the following array:

$$\begin{aligned}
\frac{dx_1}{dt} &= a_{11}x_1 + a_{12}x_2 + \dots a_{1n}x_n + z_1 \\
\frac{dx_2}{dt} &= a_{21}x_1 + a_{22}x_2 + \dots a_{2n}x_n + z_2 \\
&\vdots \\
\frac{dx_n}{dt} &= a_{n1}x_1 + a_{n2}x_2 + \dots a_{nn}x_n + z_n
\end{aligned} \tag{13}$$

Or more compactly by the following matrix differential equation:

$$\frac{d\overline{X}}{dt} = \overline{AX} + \overline{Z} \tag{14}$$

where:

$$\overline{X} = \begin{bmatrix} x_1 \\ x_2 \\ \vdots \\ x_n \end{bmatrix} \; ; \quad \overline{A} = \begin{bmatrix} a_{11}a_{12}\dots a_{1n} \\ a_{21}a_{22}\dots a_{2n} \\ \vdots \\ a_{n1}a_{n2}\dots a_{nn} \end{bmatrix} \; ; \quad \overline{Z} = \begin{bmatrix} z_1 \\ z_2 \\ \vdots \\ z_n \end{bmatrix}$$

The general incremental solution to Eq. (14) is shown in Eq. (15), followed by the simplified solution, Eq. (16), corresponding to a constant $\overline{Z}$ vector over the time interval, τ.

$$\overline{X}_{t+\tau} = e^{\overline{A}\tau}\,\overline{X}_t + e^{\overline{A}(t+\tau)} \int_t^{t+\tau} e^{-\overline{A}\tau}\,\overline{Z}_\tau\,d\tau \tag{15}$$

$$\overline{X}_{t+\tau} = e^{\overline{A}\tau}\overline{X}_t + (e^{\overline{A}\tau} - \overline{I})\,\overline{A}^{-1}\,\overline{Z}_t \tag{16}$$

where $\overline{I}$ equals the identity matrix.

The matrix exponential terms may then be approximated by the following series solutions:

$$e^{\overline{A}\tau} = \overline{I} + \overline{A}\tau + \frac{(\overline{A}\tau)^2}{2!} + \frac{(\overline{A}\tau)^3}{3!} + \ldots \frac{(\overline{A}\tau)^k}{k!} \tag{17}$$

and

$$(e^{\overline{A}\tau} - \overline{I})\overline{A}^{-1} = [\overline{A}\tau + \frac{(\overline{A}\tau)^2}{2!} + \ldots \frac{(\overline{A}\tau)^k}{k!}]\overline{A}^{-1} \tag{18}$$

or

$$(e^{\overline{A}\tau} - \overline{I})\overline{A}^{-1} = \overline{I}\tau + \frac{\overline{A}\tau^2}{2!} + \frac{\overline{A}^2\tau^3}{3!} + \ldots \frac{\overline{A}^{k-1}\tau^k}{k!} \tag{19}$$

Therefore, with given initial concentration conditions, matrix decay coefficients, and constant forcing functions, the concentration solution vector $\overline{X}$ may be determined after some time interval, τ. A digital computer may be utilized to carry out these operations for small time increments to yield the desired solution.

The half life of ^{216}Po when compared to that of ^{224}Ra and ^{212}Pb is extremely small causing its relative decay constant to be large. The MATEXP program cannot accept a range in matrix coefficients greater than 10^8. The ratio of decay constants is 2×10^6 which approaches the limit of excessive computational error. By eliminating the relatively rapid ^{216}Po decay, better computational accuracy is attained. A listing of the computer program, MATEXP, follows.

```
C     MATEXP FOR THE IBM 360/75
C
C     THIS PROGRAM CALCULATES THE SOLUTION OF A MATRIX OF FIRST
C     ORDER, SIMULTANEOUS DIFFERENTIAL EQUATIONS W/ CONSTANT COEFFICIENTS
C     OF THE FORM DX/DT = AX + Z.
C
C     THE METHOD IS PAYNTER-S MATRIX EXPONENTIAL METHOD
C
C     THE SOLUTION IS GIVEN FOR INCREMENTS OF THE INDEPENDENT
C     VARIABLE (T) FROM TZERO THROUGH TMAX
C
C     COMPUTES MATRICES C = EXP(A*T) AND
C                       HP = (C-I)*A INVERSE
C     SOLUTION X(N*T) = C*X((N-1)*T)+HP*Z((N-1)*T)
C     SERIES CALCULATION OF C AND HP MONITORED TO
C          ASSURE SPECIFIED SIGNIFICANCE.
C     IF T IS REDUCED FOR C AND HP CALCS.,
C     ORIGINAL ARGUEMENTS ARE RESTORED BY -
C          C(2*T)=C(T)*C(T)
C          HP(2*T)=HP(T)+C(T)*HP(T)
C
C     OUTPUT FROM THE PROGRAM IS PRINTED AT INTERVALS PITINC.
C     THE PROGRAM USES SUBROUTINES DISTRB AND OUTPUT
C
C     INPUT FOR THE PROGRAM CONSISTS OF
C          ONE CONTROL CARD
C          THE COEFFICIENT MATRIX A (UP TO 60 X 60)                          DIM
C          THE INITIAL CONDITION VECTOR X
C          A FIXED DISTURBANCE VECTOR Z
C
C     A VARYING Z CAN BE GENERATED BY DISTRB
C     VARIABLE COEFFICIENT EQUATIONS MAY BE SOLVED BY APPROPRIATE
C     FUDGING OF THE DISTURBANCE FUNCTION SUBROUTINE.
C
C     CONTROL CARD INPUT INFORMATION
C          NE=NO. OF EQUATIONS (I2)
C          LL=COEFF. MATRIX TAG NO.  (I2)
C          P=PRECISION OF C AND HP (F10.0) -  RECOMMEND 1.0E-6 OR LESS
C          TZERO=ZERO TIME  (F10.0)
C          T=COMPUTATION TIME INTERVAL (F10.0)
C          TMAX=MAXIMUM TIME  (F10.0)
C          PLTINC=PRINTING TIME INTERVAL (F10.0)
C          MATYES=COEFF. MATRIX (A) CONTROL FLAG (I2)
C            1=USE PREVIOUS A AND T
C            2=READ NEW COEFF.S TO ALTER A
C            3=READ ENTIRE NEW A  (NON-ZERO VALUES)
C            4=DISTRB TO CALC. ENTIRE NEW A
C            5=READ SOME, DISTRB TO CALC. OTHERS
C            6=DISTRB TO ALTER SOME A ELEMENTS
C          ICSS=INITIAL CONDITION VECTOR (XIC) FLAG (I2)
C            1=READ IN ALL NEW NON-ZERO VALUES
C            2=READ NEW VALUES TO ALTER PREVIOUS VECTOR
```

```
C            3=USE PREVIOUS VECTOR
C            4=VECTOR=0
C            5=USE LAST VALUE OF X VECTOR FROM PREVICUS RUN
C          JFLAG=FORCING FUNCTION (Z) FLAG (I2)
C            1 THRU 4=SAME AS FOR ICSS FOR CONSTANT Z
C            5=CALL DISTRB AT EACH TIME STEP FOR VARIABLE Z
C     ITMAX = MAX. NO. OF TERMS IN SERIES APPROX.
C          OF EXP(AT).  (I3)
C     LASTCC = NON-ZERO FOR LAST CASE (I1)
C     I1Z = ROW NO. OF Z IF CNLY ONE NON-ZERO,
C          OTHERWISE =0    (I2)
C     ICONTR - FOR INTERNAL CONTROL OPTIONS   (I2)
C          0=READ NEW CONTROL CARD FOR NEXT CASE
C          1=GO TO 212 CALL DISTRB FOR NEW A OR T
C         -1=GO TO 215 CALL DISTRB FOR NEW I.C.-S
C     VAR = MAX. ALLOWABLE VALUE OF LARGEST COEFF. MATRIX ELEMENT * T
C     (RECOMMEND VAR=1.0)    (F6.0)
C
      0DIMENSION A(60,60),C(60,60),HP(60,60),QPT(60,60),
      1X(60),Y(60),Z(60),XIC(60),TQP(60)
      0DIMENSION XO(60),XX(60)
      0DIMENSION PLOT1(125),PLOT2(125),PLOT3(125),PLOT4(125),PLCT5(125),
      1TIM(125)
      0DIMENSION BUFFER(4000)
C
      0COMMON C,HP,A,QPT,X,Z,Y,ITMAX,KK,IL,MM,
      1JJFLAG,XIC,NI,TIME,TMAX,TZERO,NE,TQP,T,
      2I1Z,ICONTR,PLTINC,MATYES,ICSS,JFIAG,PLT
      0COMMON XO,XX
      0COMMON PLOT1,PLOT2,PLOT3,PIOT4,PIOT5,ME,MEM1,TIM
      0COMMON BUFFER
      0COMMON JAA
C
C     K=CASE NUMBER
C     NI=0 ON 1-ST PASS.  SET TO 1 ON 1-ST CALL OF OUTPUT.
      K=1
      NI=0
      ME=0
      MEM1=0
      JAA=1
C
      READ (5,902) XO(1),XO(2),XC(3),XC(4),XO(5)
  902 FORMAT(5E12.3)
    1 READ (5,100)            NE,IL,P,TZERO,T,TMAX,PLTINC,MATYES,ICSS,
     1JFLAG,ITMAX,LASTCC,I1Z,ICONTR,VAR
  100 FORMAT(2(I2,3X),5F10.0,3I2,I3,I1,2I2,F6.0)
C
C     COEFFICIENT MATRIX INPUT
      GO TO (3,99,2,2,2,3),MATYES
C
    2 DO 90 I=1,NE
      DO 90 J=1,NE
   90 A(I,J)=0.0
      IF(MATYES-4)99,3,99
   99 DO 91 I=1,1379
```

```
C       MATRIX ELEMENTS  4(ROW, COLUMN, VALUE)
C       ALL I AND J ENTRIES ON CARD MUST BE NON-ZERO.
C       A BLANK CARD IS REQUIRED AFTER ALL ELEMENTS ARE READ IN.
        READ (5,101)            I1,J1,D1,I2,J2,D2,I3,J3,D3,I4,J4,D4
 101    FORMAT (4(2I3,E12.3))
C
        IF(I1)3,3,92
   92   A(I1,J1)=D1
        A(I2,J2)=D2
        A(I3,J3)=D3
 91     A(I4,J4)=D4
C
C       INITIAL CONDITION VECTOR XIC INPUT
     3  GO TO(4,120,6,5,6),ICSS
C
     4  DO 93 I=1,NE
    93  XIC(I)=0.0
   120  DO 94 I=1,15
C       ALL ROW (I) ENTRIES MUST BE NON-ZERO
C       A BLANK CARD IS REQUIRED AFTER ALL ELEMENTS ARE READ IN.
        READ (5,95)             MM,I11,D11,I12,D12,I13,D13,I14,D14,I15,D15
   95   FORMAT(I2,5(I3,E12.3))
        IF (I11)6,6,96
    96  XIC(I11)=D11
        XIC(I12)=D12
        XIC(I13)=D13
        XIC(I14)=D14
   94   XIC(I15)=D15
C
     5  MM=0
        DO 7 I=1,NE
     7  XIC(I)=0.0
     6  IF(ICSS-5)81,214,81
    81  DO 82 I=1,NE
    82  X(I)=XIC(I)
   214  IF(MATYES-3)213,213,212
   212  CALL DISTRB
   213  JJFLAG=0
C       QPTMP = MAX. PERMISSIBLE ELEMENT OF QPT FOR  8 DECIMAL COMPUTER
C       MATRIX CALC. LOSES SIGNIFICANCE IF LARGEST
C         ELEMENT IN SERIES APPROX. MATRIX QPT IS
C         GREATER THAN P*1.0E8
        QPTMP=P*1.0E8
C
        WRITE (6,211)           K,NE,P,T,
       1PLTINC,MATYES,ICSS,JFLAG,ICONTR,ITMAX,I1Z,VAR,QPTMP
C
  2110FORMAT(12H1MATEXP CASE,I3/17H NO. OF EQUATIONS,
       1I3/20H SPECIFIED PRECISION,F12.8/6H TIME ,
       28HINTERVAL,F18.8/15H PLOT INCREMENT,F17.8//
       316H CONTROL FLAGS -/1H ,5X,6HMATYES,I4/1H ,
       45X,4HICSS,I6/1H ,5X,5HJFLAG,I5/1H ,5X,6HICONTR,I4/
       534HOMAX. TERMS IN EXPONENTIAL APPROX.,I5/
       613H SINGLE Z ROW,I4/20H MAX. ALLOWABLE A*DT,F9.3/
       727H MAX. ALLOWABLE QPT ELEMENT,F11.3)
```

```
C
      PLTINC=PLTINC*0.9999
C
      JFK=0
      IF(MATYES-1)20,20,806
C     SCAN MATRIX FOR MAX. AND MIN. NON-ZERO ELEMENTS.
 806  IMAX=1
      JMAX=1
      AMAX=ABS (A(1,1))
      DO 401 I=1,NE
      DO 401 J=1,NE
      IF(AMAX-ABS (A(I,J)))402,401,401
 402  AMAX=ABS (A(I,J))
      IMAX=I
      JMAX=J
 401  CONTINUE
      IMIN=IMAX
      JMIN=JMAX
      AMIN=AMAX
      DO 409 I=1,NE
      DO 409 J=1,NE
      IF(A(I,J)) 407,409,407
 407  IF(ABS (A(I,J))-AMIN) 408,409,409
 408  AMIN=ABS (A(I,J))
      IMIN=I
      JMIN=J
 409  CONTINUE
C     AMIN = MINIMUM NON-ZERO ELEMENT
      ISTOR=0
      ADT=AMAX*T
      DO 403 I=1,11
      IF(VAR-ADT) 413,404,404
  413 ISTOR=ISTOR+1
 403  ADT=ADT*0.5
 404  T=ADT/AMAX
C     COMPUTATION INTERVAL T IS HALVED ISTOR
C       TIMES (10=MAX.) SO MAX. ELEMENT IN A*T
C       IS LESS THAN VAR.
      WRITE (6,405)            IMAX,JMAX,A(IMAX,JMAX),ADT,T,
     1 IMIN,JMIN,A(IMIN,JMIN)
 405  FORMAT (31H0MAX.COEFF. MATRIX ELEMENT = A(,I2,1H,,I2,3H) =,
     1 E15.4/13H MAX. A*DT = ,F12.8,2X,14HWITH DELTA T =,F15.8/
     230H0MINIMUM NON-ZERO ELEMENT = A(,I2,1H,,I2,3H) =,E15.4)
      RATIO=AMAX/AMIN
      WRITE(6,450) RATIO
 450  FORMAT(18H0RATIO AMAX/AMIN =,E15.4)
C
      IF(ISTOR-10)8,410,410
  410 WRITE (6,411)
  4110FORMAT(34H0A*DT STILL GREATER THAN ALLOWABLE,
     119H AFTER 10 HALVINGS.)
      GO TO 37
C     CALCULATION OF MATRIX EXPONENTIALS C AND HF
    8 DO 9 I=1,NE
      DO 9 J=1,NE
```

```
    9 C(I,J)=0.
C
      DO 10 I=1,NE
   10 C(I,I)=1.
C
C     SKIP HP CALCS. FOR HOMOGENEOUS EQUATIONS
      IF (JFLAG-4)48,51,48
   48 DO 49 I=1,NE
      DO 49 J=1,NE
   49 HP(I,J)=0.
C
      DO 50 I=1,NE
   50 HP(I,I)=T
C
   51 PE=0.0
C
      DO 11 I=1,NE
      DO 11 J=1,NE
  11  QPT(I,J)=C(I,J)
C
C NOW FORM THE MATRIX EXPONENTIALS C=EXP(A*T) AND HP=((C-I)*A INVERSE)
C
      AL=1.0
C
   12 DO 16 KL=1,ITMAX
C
      KLM=KL
      ALL=T/AL
      AL=AL+1.0
      TALLL=T/AL
C
      DO 18 I=1,NE
C
C
      DO 13 J=1,NE
      TQP(J)=0.0
      DO 13 KX=1,NE
  13  TQP(J)=TQP(J)+QPT(I,KX)*A(KX,J)
C
      DO 18 J=1,NE
  18  QPT(I,J)=TQP(J)*ALL
C
C     QPT=MATRIX TERM IN SERIES APPROX. =((A*T)**K)/K FACTORIAL
C
      DO 44 I=1,NE
      DO 44 J=1,NE
   44 C(I,J)=C(I,J)+QPT(I,J)
C
      IF (JFLAG-4)45,47,45
C
  45  IF(ITMAX-KL)47,47,145
  145 DO 46 I=1,NE
      DO 46 J=1,NE
   46 HP(I,J)=HP(I,J)+QPT(I,J)*TALLL
C
```

```
C
C FIND MAX ABS ELEMENT IN QPT AND CALL IT PMK
C
C     LARGEST QPT ELEMENT USUALLY IN ROW IMAX, COLUMN JMAX
  47  PMK=ABS (QPT(IMAX,JMAX))
      IF(QPTMP-PMK) 83,83,502
 502  IF(PMK-P) 406,406,16
C     SCAN OTHER QPT ELEMENTS ONLY WHEN QPT(IMAX, JMAX) IS LESS THAN P
 406  DO 14 I=1,NE
      DO 14 J=1,NE
  14  PMK=AMAX1(PMK,ABS (QPT(I,J)))
      IF(PMK-P)17,17,16
C
C     PRESENT MAX. QPT ELEMENT SHOULD BE LESS THAN
C       HALF PREVIOUS MAX. TO INSURE CONVERGENCE
   17 IF(PE-2.*PMK)16,21,21
   16 PE=PMK
C
  21  WRITE (6,200)            KLM
C
  200 FORMAT(44H0NO. OF TERMS IN SERIES APPROX. OF MATEXP = ,I2)
C
      IF(ITMAX-1)20,20,538
  538 IF(KLM-ITMAX) 414,83,83
C
  83  T=T*0.5
      JFK=JFK+1
      IF(JFK-7)303,304,304
 304  WRITE (6,305)            PMK
 305 0FORMAT(32H07 TRIES AT HALVING T N.G., PMK=,F12.6)
      GO TO 37
 303  WRITE (6,210)            KLM,PMK,T
 210  FORMAT(21H0MAX. ELEMENT IN TERM,I3,8HOF QPT =,E11.3/
     1 35H TRY HALVED TIME INTERVAL DELTA T =,F15.8)
      GO TO 8
  414 ISTOR=ISTOR+JFK
C     ORIGINAL ARGUMENTS OF C AND HP MATRICES RESTORED IF ISTOR GREATER THAN 0
      IF(ISTOR) 20,20,416
  416 WRITE (6,415)            ISTOR
  415 FORMAT(26H0TOTAL NO. OF T HALVINGS =,I3)
      DO 417 KR=1,ISTOR
      IF(JFLAG-4) 419,418,419
C     SKIP HP CALCS. FOR HOMOGENEOUS EQUATIONS
  419 DO 420 I=1,NE
      DO 421 J=1,NE
      TQP(J)=0.0
      DO 421 KX=1,NE
  421 TQP(J)=TQP(J)+HP(I,KX)*C(KX,J)
      DO 420 J=1,NE
  420 HP(I,J)=TQP(J)+HP(I,J)
C
  418 DO 430 I=1,NE
      DO 430 J=1,NE
  430 QPT(I,J)=0.0
      DO 431 I=1,NE
```

```
      DO 431 J=1,NE
      DO 431 KX=1,NE
  431 QPT(I,J)=QPT(I,J)+C(I,KX)*C(KX,J)
      DO 432 I=1,NE
      DO 432 J=1,NE
  432 C(I,J)=QPT(I,J)
 417  T=2.0*T
C
C     C(I,J) IS THE MATRIX EXPONENTIAL C=EXP(A*T)
C     AND HP(I,J) IS THE ((C-I)*A INVERSE) MATRIX
C NOW WE READ (OR CALL SUBROUTINE FOR) DISTURBANCE VECTOR
C
C
   20 TIME=TZERO
      PLT=0.
      GO TO (26,121,27,25,55),JFIAG
   55 IF(MATYES-3)215,215,27
  215 CALL DISTRB
      I1Z=I1Z
      GO TO 27
C
   26 DO 97 I=1,NE
   97 Z(I)=0.0
  121 DO 98 I=1,15
C     ALL ROW (I) ENTRIES MUST BE NON-ZERO
C     A BLANK CARD IS REQUIRED AFTER ALL ELEMENTS ARE READ IN.
      READ (5,95)            KK,I21,D21,I22,D22,I23,D23,I24,D24,I25,D25
      IF(I21)27,27,78
   78 Z(I21)=D21
      Z(I22)=D22
      Z(I23)=D23
      Z(I24)=D24
  98  Z(I25)=D25
C
   25 KK=0
      DO 28 I=1,NE
   28 Z(I)=0.
C
C     ON 1-ST CALL OF OUTPUT NI SET TO 1
   27 CALL OUTPUT
C
C NOW COMES THE EQUATION SOLUTION BASED ON
C     X(NT)=M*X(NT-1)+((M-I)A INV.)*Z(NT-1)
C
   24 IF (JFLAG-4)29,54,56
   54 DO 53 I=1,NE
      Y(I)=C(I,1)*X(1)
      DO 53 J=2,NE
   53 Y(I)=Y(I)+C(I,J)*X(J)
      IF(I1Z)52,52,702
   56 IF(JJFLAG)30,29,30
   30 CALL DISTRB
   29 IF(I1Z)700,700,54
C     ONLY ONE Z-TERM CALC. IF I1Z IS GREATER THAN ZERO
  702 DO 703 I=1,NE
```

```
  703 Y(I)=Y(I)+HP(I,I1Z)*Z(I1Z)
      GO TO 52
  700 DO 32 I=1,NE
      Y(I)=C(I,1)*X(1)+HP(I,1)*Z(1)
      DO 32 J=2,NE
   32 Y(I)=Y(I)+C(I,J)*X(J)+HP(I,J)*Z(J)
   52 DO 31 I=1,NE
   31 X(I)=Y(I)
C
C ONE TIME INCREMENT OF THE SOLUTION HAS JUST BEEN FOUND
C
C NOW PLOT AND PRINT IF PLTINC INTERVAL HAS ELAPSED
C
      JJFLAG=1
      TIME=TIME+T
      PLT=PLT+T
      IF(PLT-PLTINC)35,33,33
   33 CALL OUTPUT
      PLT=0.
   35 IF(TIME-TMAX)24,37,37
  37  IF(LASTCC)40,34,40
   34 K=K+1
      NI=0
      PLT=0.0
      IF(ICONTB)215,1,212
   40 CONTINUE
      MEM1=ME-1
      CALL FIXPLT(0.00,25.0,0.00,100.0,'LINEAR','MECH',0.,0.,BUFFER,
     14000,'HHF PLOT$')
      GO TO (932,932,932,932,933,933,933,933,934,935,936),JAA
  932 CALL TITLE(0.4,'RA DECAY CHAIN WITH RN RELEASE$','TIME, HRS$',
     1'RELATIVE CONCENTRATION, PERCENT$')
      GO TO 938
  933 CALL TITLE(0.4,'RA DECAY CHAIN WITH RA RELEASE$','TIME, HRS$',
     1'RELATIVE CONCENTRATION, PERCENT$')
      GO TO 938
  934 CALL TITLE(0.4,'RA DECAY CHAIN WITH PB RELEASE$','TIME, HRS$',
     1'RELATIVE CONCENTRATION, PERCENT$')
      GO TO 938
  935 CALL TITLE(0.4,'RA DECAY CHAIN WITH BI RELEASE$','TIME, HRS$',
     1'RELATIVE CONCENTRATION, PERCENT$')
      GO TO 938
  936 CALL TITLE(0.4,'RA DECAY CHAIN WITH TL RELEASE$','TIME, HRS$',
     1'RELATIVE CONCENTRATION, PERCENT$')
  938 CALL RAYPLT(TIM,PLOT1,MEM1)
      CALL RAYPLT(TIM,PLOT2,MEM1)
      CALL RAYPLT(TIM,PLOT3,MEM1)
      CALL RAYPLT(TIM,PLOT4,MEM1)
      CALL RAYPLT(TIM,PLOT5,MEM1)
      CALL ADVANS
      JAA=JAA+1
      ME=0
      MEM1=0
      K=1
      NI=0
```

```
      IF(JAA-12) 1,920,920
  920 CONTINUE
      STOP
      END
      SUBROUTINE OUTPUT
C
C
     0DIMENSION A(60,60),C(60,60),HP(60,60),QPT(60,60),
     1X(60),Y(60),Z(60),XIC(60),TQP(60)
     0DIMENSION XO(60),XX(60)
     0DIMENSION PLOT1(125),PLOT2(125),PLOT3(125),PLOT4(125),PLOT5(125),
     1TIM(125)
     0DIMENSION BUFFER(4000)
C
     0COMMON C,HP,A,QPT,X,Z,Y,ITMAX,KK,LL,MM,
     1JJFLAG,XIC,NI,TIME,TMAX,TZERO,NE,TQP,T,
     2I1Z,ICONTR,PLTINC,MATYES,ICSS,JFLAG,PLT
     0COMMON XO,XX
     0COMMON PLOT1,PLOT2,PLOT3,PLOT4,PLOT5,ME,MEM1,TIM
     0COMMON BUFFER
     0COMMON JAA
C
      IF(NI) 2,1,2
    1 NI=1
      NC=10
      DO 11 NCM=1,51,10
      WRITE(6,200) LL,((A(I,J),J=NCM,NC),I=1,NE)
  200 FORMAT (2H0A,I2/(1H ,1P10E11.3))
      IF(NE-NC) 10,10,11
  11  NC=NC+10
C
  10  NC=10
      DO 21 NCM=1,51,10
      WRITE(6,201) ((C(I,J),J=NCM,NC),I=1,NE)
  201 FORMAT (2H0C/(1H ,1P10E11.3))
      IF(NE-NC) 20,20,21
  21  NC=NC+10
C
 20   IF(JFLAG.EQ.4) GO TO 2
      NC=10
      DO 31 NCM=1,51,10
      WRITE(6,202) ((HP(I,J),J=NCM,NC),I=1,NE)
  202 FORMAT (3H0HP/(1H ,1P10E11.3))
      IF(NE-NC) 3,3,31
  31  NC=NC+10
C
  3   IF(JFLAG.NE.5) WRITE (6,204) (Z(I),I=1,NE)
    2 DO 903 I=1,NE
  903 XX(I)=(X(I)/XO(I))*100.0
      IF(ME.EQ.0) GO TO 910
      TIM(ME)=TIME
      IF(ME.GT.125) GO TO 910
      PLOT5(ME)=XX(5)
      PLOT4(ME)=XX(4)
      PLOT3(ME)=XX(3)
```

```
      PLOT2(ME)=XX(2)
      PLOT1(ME)=XX(1)
  910 ME=ME+1
      WRITE(6,203) TIME,(XX(I),I=1,NE)
  203 FORMAT(4H T =,1PE10.3,4H X =,       /(1H ,5X,10E11.3))
      IF(JFLAG.NE.5) GO TO 30
      WRITE(6,204) (Z(I),I=1,NE)
  204 FORMAT(6H Z =  ,1P10E11.3/(1H ,5X,10E11.3))
   30 RETURN
      END
      SUBROUTINE DISTRB
     0DIMENSION A(60,60),C(60,60),HP(60,60),QPT(60,60),
     1X(60),Y(60),Z(60),XIC(60),TQP(60)
     0COMMON C,HP,A,QPT,X,Z,Y,ITMAX,KK,LL,MM,
     1JJFLAG,XIC,NI,TIME,TMAX,TZERO,NE,TQP,T,
     2I1Z,ICONTR,PLTINC,MATYES,ICSS,JFIAG,PLT
     0COMMON JAA
C
   30 RETURN
      END
```

9.2 Experimental Data

The original data can be found in ORNL databooks listed in Appendix 9.5. A summary of experimental conditions and reference samples is given in Table 7.

9.3 Porosimetry Measurements

Mercury, due to its high surface tension, does not penetrate small pores unless pressure is applied. The pressure necessary to force mercury into pores of mean radius $\bar{a}$ is related to the radius as:

$$\pi \bar{a}^2 p = -2\pi \bar{a} \sigma' \cos\theta \tag{20}$$

or

$$\bar{a} = -\frac{2\sigma' \cos\theta}{p} \tag{21}$$

Thus,

$$\bar{a}(\mathring{A}) = \frac{1.75 \times 10^6}{p} \tag{22}$$

where:

θ = contact angle between mercury and the pore wall

p = pressure, psi

σ' = surface tension of mercury

$\bar{a}$ = mean pore radius

By increasing pressure slowly and measuring the total volume of mercury forced into pores, one obtains a graph of cumulative pore volume versus radius such as those of Figs. 21 and 22 for uncarbonized and carbonized resin beads, respectively.

9.4 Sample Calculations

9.4.1 Equilibrium Concentrations of ^{232}U Decay Chain

The loaded resin is 32% by weight uranium, and this uranium contains 100-1500 ppm ^{232}U as impurity (4). For the worst case, that of 1500 ppm ^{232}U, the concentration of ^{232}U in the uranium-loaded resin is

Table 7. Reference Sample Activity

	Run 199		Run 200		Run 201		Run 202		Run 203		Run 204	
	Time (hr)	Activity (GPS)*	Time (hr)	Activity (GPS)	Time (hr)	Activity (GPS)	Time (hr)	Activity (GPS)	Time (hr)	Activity (GPS)	Time (hr)	Activity (GPS)
	71	1445	77	1408	74	1443	76	1514	77	1506	76	1503
	100	1424	96	1446	97	1484	100	1515	98	1498	101	1516
	103	1409	120	1467	122	1482	122	1461			102	1511
	119	1444	145	1447	147	1489	125	1524				
	142	1443	170	1425								
	190	1455	195	1448								
	218	1445										
Average Activity (GPS)		1438		1440		1475		1504		1502		1510
Furnace Temperature (°C)		800		400		600		500		700		1000

*GPS denotes gamma emissions per second per gram ^{232}Th.

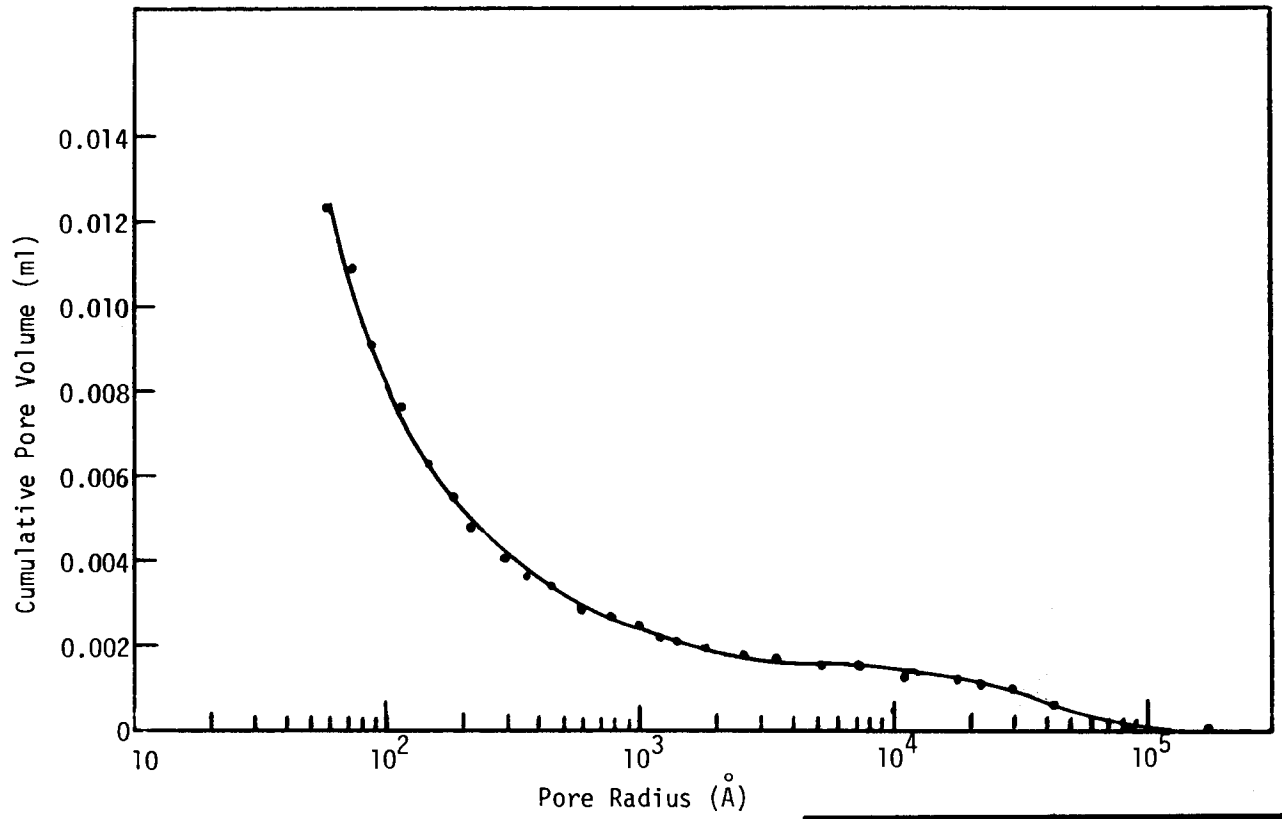

sample volume = 0.200 ml

MASSACHUSETTS INSTITUTE OF TECHNOLOGY
SCHOOL OF CHEMICAL ENGINEERING PRACTICE
AT
OAK RIDGE NATIONAL LABORATORY

CUMULATIVE PORE VOLUME VS MEAN PORE RADIUS FOR UNCARBONIZED BEADS

DATE	DRAWN BY	FILE NO.	FIG.
12-14-74	SAR	CEPS-X-206	21

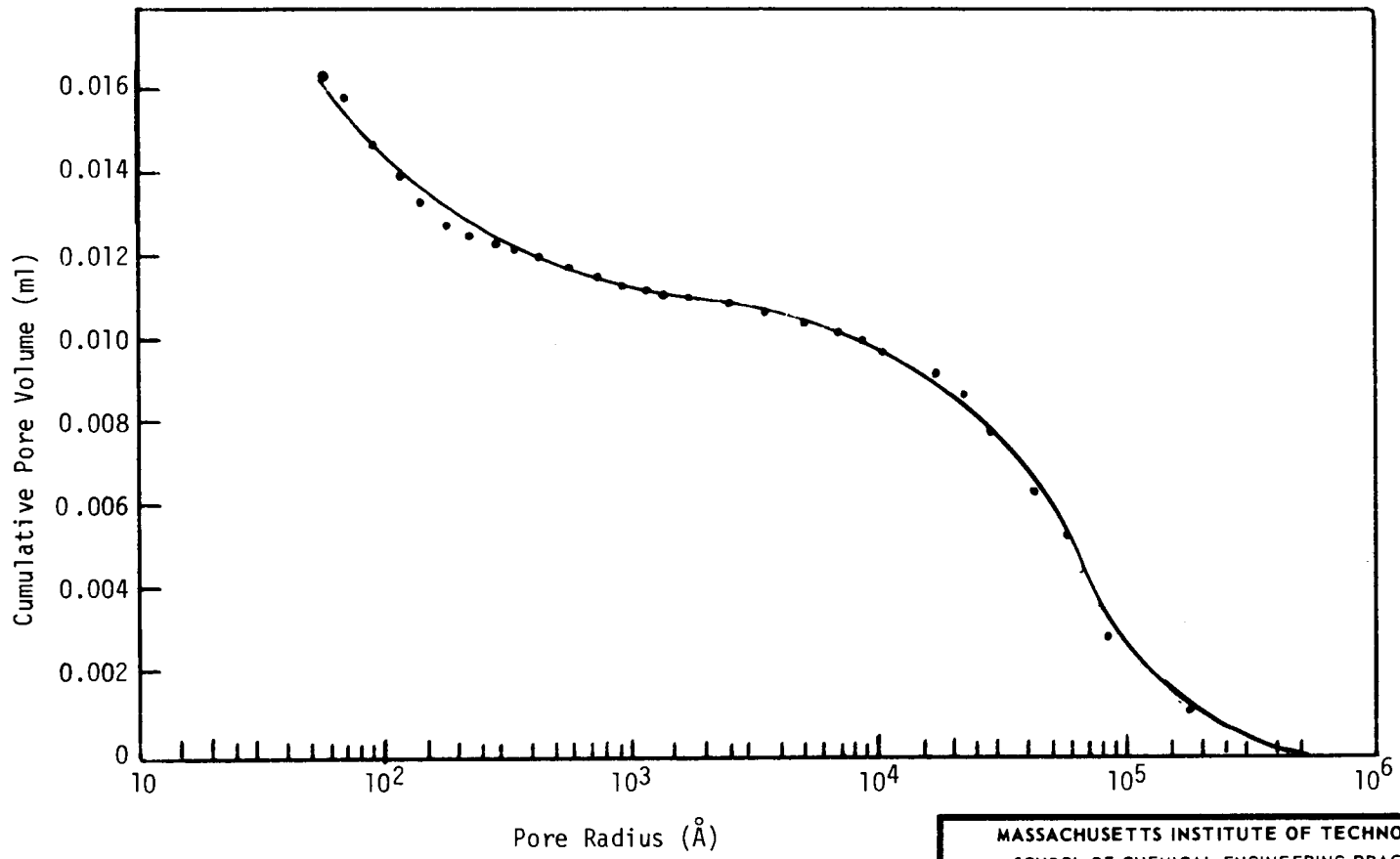

sample volume = 0.200 ml

MASSACHUSETTS INSTITUTE OF TECHNOLOGY
SCHOOL OF CHEMICAL ENGINEERING PRACTICE
AT
OAK RIDGE NATIONAL LABORATORY

CUMULATIVE PORE VOLUME VS MEAN PORE RADIUS FOR CARBONIZED (600°C) BEADS

DATE	DRAWN BY	FILE NO.	FIG.
12-14-74	SAR	CEPS-X-206	22

$$\frac{g\ ^{232}U}{g\ resin} = \frac{32\ g\ U}{100\ g\ resin} \times \frac{1500\ g\ ^{232}U}{10^6\ g\ U} = 4.8 \times 10^{-4}\ g\ ^{232}U/g\ resin$$

The density of the resin is approximately 1 g/cm^3 or 5890 beads/cm^3. Therefore, the molar concentration of ^{232}U per bead is

$$\frac{moles\ ^{232}U}{bead} = \frac{4.8 \times 10^{-4}\ g\ ^{232}U/cc}{232\ g/gmole} \times \frac{1\ cc}{5890\ beads}$$

$$= 3.5 \times 10^{-10}\ moles\ ^{232}U/bead$$

Equilibrium concentrations of the daughters in the chain can now be obtained using the above ^{232}U concentration, since at equilibrium:

$$\lambda_p[P] = \lambda_D[D] \tag{23}$$

$$\lambda_i = \frac{\ln 2}{t_{1/2,i}} \tag{24}$$

$$[D] = \frac{t_{1/2,D}}{t_{1/2,P}} \times [P] \tag{25}$$

9.4.2 <u>^{232}Th Decay Rate</u>

The concentration of ^{232}Th changes insignificantly compared with its daughter products since its half-life is many orders of magnitude larger. The ^{232}Th decay rate is:

$$\frac{-d[^{232}Th]}{dt} = \frac{\ln 2}{t_{1/2}}[^{232}Th] = \frac{0.693[^{232}Th]}{(1.39 \times 10^{10}\ yr)(3.154 \times 10^7\ sec/yr)}$$

$$= 1.58 \times 10^{-18}\ [^{232}Th]\ sec^{-1}$$

The concentration of ^{232}Th in moles/bead can be determined knowing that the density of unheated beads loaded with 32% ^{232}Th by weight is approximately 1 g/cc; the number of moles of ^{232}Th per cc of beads is

$$\frac{(1\ g/cc)(0.32\ g\ ^{232}Th)}{232\ g\ Th/mole\ Th} = 1.38 \times 10^{-3}\ moles\ Th/cc$$

The number of beads per cc is

$$\frac{1}{cc/bead}(1 - \text{void fraction between beads}) = \frac{6}{\pi d^3}(1 - f_v)$$

The beads are 28 mesh, or 0.0595 cm in diameter, and from Perry (5), $f_v = 0.35$. Thus,

$$\text{no. of beads/cc} = \frac{6(0.65)}{\pi(0.0595)^3} = 5.89 \times 10^3$$

Thus, the amount of ^{232}Th is

$$\frac{1.38 \times 10^{-3}\ moles/cc}{5.89 \times 10^3\ beads/cc} = 2.34 \times 10^{-7}\ moles/bead$$

Therefore, the ^{232}Th decay rate is:

$$(1.58 \times 10^{-18})(2.34 \times 10^{-7}) = 3.70 \times 10^{-25}\ moles/bead\text{-}sec$$

$$(3.70 \times 10^{-25})(6.02 \times 10^{23}) = 0.22\ atoms/sec\text{-}bead$$

This is the rate of decay and of formation of all the daughter products when the decay chain is in secular equilibrium.

The ratio of ^{232}U to ^{232}Th activity for equal amounts of ^{232}U and ^{232}Th loaded onto separate batches of resin is:

$$\frac{^{232}U\ decay\ rate}{^{232}Th\ decay\ rate} = \frac{t_{1/2,Th}}{t_{1/2,U}} \times \frac{[^{232}U]}{[^{232}Th]} = \frac{[3.5 \times 10^{-10}][1.39 \times 10^{10}]}{[2.34 \times 10^{-7}][72]}$$

$$= 2.9 \times 10^5$$

9.4.3 Daughter Product Concentrations at Secular Equilibrium

At secular equilibrium or steady state,

$$\frac{d[D]}{dt} = 0$$

and

$$\lambda_P[P] = \lambda_D[D] \tag{23}$$

The concentrations of all species in the decay chain are inversely proportional to the decay constant which is inversely proportional to the half-life. Consequently, using the thorium concentration, 2.34×10^{-7} moles Th/bead, the concentration of ^{220}Rn at equilibrium is

$$(2.34 \times 10^{-7}) \times t_{1/2,^{220}Rn}/t_{1/2,^{232}Th}$$

$$= \frac{(2.34 \times 10^{-7})(54.5 \text{ sec})}{(1.39 \times 10^{10} \text{ yr})(3.154 \times 10^{7} \text{ sec/yr})}$$

$$= 2.91 \times 10^{-23} \text{ moles } ^{220}Rn/\text{bead}$$

The concentrations of the other daughter species at steady state are listed in Table 4 of Sect. 5.

9.4.4 Theoretical Self-Shielding Effects

The degree of gamma ray attenuation (self-shielding) effects can be calculated using the equation

$$Q_T = \exp(-\sum_i N_i \rho_i x) \tag{12}$$

The diameter of a sample holder is 1 cm. Thus, to penetrate the sample, a gamma ray must travel approximately 0.5 cm. Before heating, the beads have a density of 1 g/cc and are loaded with 32% ^{232}Th by weight. The density of oxygen and nitrogen accompanying thorium can be calculated using a stoichiometry of $[ThO_2(NO_3) \cdot \text{resin}]$ for the adsorbed thorium. Thus, the amounts of Th, O, and N in one gram of unheated resin are 0.320, 0.110, and 0.019 gm. The remaining 0.551 gm is resin material which is approximately $C_6H_6O_2$. Thus, the resin contributes 0.342, 0.057, and 0.152 gm of C, H, and O, respectively. Combining the above factors to determine apparent component

density, the densities of Th, O, N, C, and H are 0.320, 0.262, 0.019, 0.342, and 0.057, respectively. Gamma ray mass attenuation factors were obtained at 583 keV and 2615 keV (8). The mass attenuation factor for thorium was not reported so that the mass attenuation factor for uranium was used as an approximation.

From the above data, the total transmission was determined to be

$$Q_T = 0.9484 \text{ at } 583 \text{ keV}$$

and

$$Q_T = 0.9786 \text{ at } 2615 \text{ keV}$$

for the unheated resin.

If it is assumed that only ThO_2 and C remained after the heating process, the density of Th, O, and C were found to be 0.906, 0.124, and 0.969, respectively. The resultant total transmission was

$$Q_T = 0.8962 \text{ at } 583 \text{ keV}$$

and

$$Q_T = 0.9587 \text{ at } 2615 \text{ keV}$$

for the heated resin.

If the percent difference is defined as

$$\% \text{ difference} = \frac{Q_{T,\text{unheated}} - Q_{T,\text{heated}}}{Q_{T,\text{unheated}}} \times 100\%$$

then the

$$\% \text{ difference at } 584 \text{ keV} = \frac{0.9484 - 0.8962}{0.9484} \times 100\% = 5.5\%$$

and

$$\% \text{ difference at } 2615 \text{ keV} = \frac{0.9786 - 0.9587}{0.9786} \times 100\% = 2.0\%$$

Since the total gamma activity of the sample is measured as the sum of the activities at both gamma energies, the two percentages are weighted according to the approximate contributions of each energy to the total

activity. For a total activity of 1400 GPS, 800 counts are at 2615 keV and 600 counts are at 538 keV, so that

$$\text{weighted \% difference} = 5.5\left(\frac{600}{1400}\right) + 2.0\left(\frac{800}{1400}\right) = 3.5\%$$

It should be noted that many assumptions have been made in this calculation and that the result may be inaccurate by a factor of two.

9.4.5 Background Count

The sample container in Run IE-202 gave net counts of 48 and 10 in the markers corresponding to 583 and 2615 keV. The counting time in each case was 4000 sec. Therefore,

$$CPS_{583} = 6.75 \times 10^{-3}$$

$$CPS_{2615} = 2.50 \times 10^{-3}$$

Counts per second can be converted to gammas per second (GPS) using the detector efficiency f_E, a function of geometry and gamma energy. If we use the results of a later count taken on the resin used in Run IE-202, these efficiencies can be calculated. At 583 keV, the reading obtained from the sample was:

$$GPS = 625.0$$

$$CPS = 2.259$$

$$f_{583} = \frac{GPS}{CPS} = \frac{625.0}{2.259} = 276.7$$

At 2615 keV, the reading obtained was:

$$GPS = 791.1$$

$$CPS = 0.6285$$

so

$$f_{2615} = 1258.7$$

Therefore,

$$GPS_{583} = CPS_{583} \times f_{583} = (6.75 \times 10^{-3})(276.7) = 1.87$$

$$GPS_{2615} = CPS_{2615} \times f_{2615} = (2.50 \times 10^{-3})(1258) = 3.15$$

9.4.6 Gamma-Detector Errors

The gamma-ray detection system was the source of two experimental errors. First, error in the measurement of the distance between source and detector resulted in a maximum counting error of 4%. The distance could be measured to within one millimeter. Since the desired distance was 5 cm and since the number of counts recorded is inversely proportional to the square of the distance, the error associated with a one millimeter discrepancy was:

$$\text{error} = \frac{(51\ \text{mm})^2 - (50\ \text{mm})^2}{(50\ \text{mm})^2} \times 100 = 4.0\%$$

The second source of error involved the statistics of measuring the frequency of decay. Since the decay of an atom is a random event, the statistical measurement of mean activity is governed by the binomial distribution (2). Since the thallium concentration is nearly constant over one counting period, the standard deviation of the measurement of the mean is approximately equal to the square root of the mean itself. Since error arises in the determination of both the background radiation and the net radiation due to the sample itself, the variances of each must be added to obtain the total variance:

$$\sigma^2_{total} = \sigma^2_{net\ counts} + \sigma^2_{baseline} = \text{gross counts} + \text{baseline counts}$$

The percent error in counts at 95% confidence is then calculated as

$$\%\ \text{error} = 1.96 \frac{\sqrt{\text{gross counts} + \text{baseline counts}}}{\text{net counts}}$$

$$= 1.96 \frac{\sqrt{\text{gross counts} + \text{baseline counts}}}{\text{gross counts} - \text{baseline counts}}$$

A PDP-11 computer program interfaced to the detector automatically calculates the standard deviation and reports the percent error at 3σ (99.73% confidence); this error was in the range 2-5% for all samples.

Errors due to incomplete filling of the sample rabbits were eliminated by using the same heated sample as the reference.

9.5 Location of Original Data

The original data are located in ORNL Databook A-7216-G, pp. 1-10, and Databook A-7214-G, pp. 1-100, on file at the MIT School of Chemical Engineering Practice, Bldg. 3001, ORNL.

9.6 Nomenclature

a_i	an element of $\bar{A}$
$\bar{a}$	mean pore radius, Å
$\bar{A}$	matrix of coefficients
CPS	counts per second
d	diameter, cm
D	daughter nuclide
f_E	detector efficiency
f_V	void fraction between particles
GPS	gamma emissions per second
$\bar{I}$	identity matrix
λ	decay constant
m	density of nuclide
N_i	mass attenuation coefficient of species i, cm^2/gm
P	parent nuclide
p	pressure, psi
ρ	density, gm/cc
Ø	ratio of ^{232}U to ^{232}Th activities
Q	attenuation
Q_T	total attenuation

σ standard deviation

τ time interval

σ' surface tension, dynes/cm

θ contact angle, degrees

t independent variable, time

$t_{1/2}$ half-life

x_i an element of $\overline{X}$

x thickness, cm

$\overline{X}$ vector of dependent variables

Z_i forcing function or element of $\overline{Z}$

$\overline{Z}$ vector of forcing functions

[ ] concentration of a nuclide

9.7 Literature References

1. Ball, S.J., and R.K. Adams, "MATEXP: A General Purpose Digital Computer Program for Solving Ordinary Differential Equations by the Matrix Exponential Method," ORNL-TM-1933 (August 30, 1967).

2. Dyer, F.F., personal communication, December 2, 1974.

3. Hamby, C., personal communication, ORNL, December 4, 1974.

4. Jenkins, J.D., S.R. McNeany, and J.E. Rushton, "Special Nuclear Assay and Accountability System for the HTGR Fuel Refabrication Pilot Plant," Sects. 2 and 4, ORNL (November 1974).

5. Perry, R.H., C.H. Chilton, and S.D. Kirkpatrick, "Chemical Engineers' Handbook," 4th ed., p 5-51, McGraw-Hill, New York (1963).

6. Rushton, J.E., personal communication, ORNL, December 12, 1974.

7. Standen, A., ed., "Kirk-Othmer Encyclopedia of Chemical Technology," Vol. 3, pp. 527-547, Vol. 1, p. 351, Vol. 12, pp. 266-298, Vol. 20, pp. 248-258, Interscience Publishers, New York (1964).

8. United States Atomic Energy Commission, "Reactor Physics Constants," ANL-5800, 2nd ed., pp. 651-652, USAEC (July 1963).

9. Weast, R.C., ed., "Handbook of Chemistry and Physics," 47th ed., p. D-100, The Chemical Rubber Co., Cleveland, Ohio (1966).

ORNL-MIT-206

INTERNAL DISTRIBUTION

1. R.L. Beatty
2. R.A. Bradley
3. W.P. Eatherly
4. J.D. Jenkins
5. P.R. Kasten
6. C.E. Lamb
7. A.L. Lotts
8-12. S.R. McNeany
13. A.R. Olsen
14. M.E. Pruitt
15. G.D. Robbins
16. J.E. Rushton
17-18. Central Research Library
19. Document Reference Section
20-22. Laboratory Records
23. Laboratory Records, ORNL R.C.
24. ORNL Patent Office
25-39. M.I.T. Practice School

EXTERNAL DISTRIBUTION

40. D.B. Anthony, MIT
41. J.E. Vivian, MIT